

**Review article**

## Self-assembly of DNA-functionalized colloids

P.E. Theodorakis<sup>1</sup>, N.G. Fytas<sup>2</sup>, G. Kahl<sup>3,4</sup>, Ch. Dellago<sup>4,5</sup>

<sup>1</sup> Department of Chemical Engineering, Imperial College London, South Kensington Campus, SW7 2AZ London, UK

<sup>2</sup> Applied Mathematics Research Centre, Coventry University, CV1 5FB, Coventry, UK

<sup>3</sup> Institute for Theoretical Physics, Vienna University of Technology, Wiedner Hauptstraße 8–10, A-1040 Vienna, Austria

<sup>4</sup> Center for Computational Materials Science (CMS), Wiedner Hauptstraße 8–10, A-1040 Vienna, Austria

<sup>5</sup> Faculty of Physics, University of Vienna, Boltzmanngasse 5, A-1090 Vienna, Austria

Received January 21, 2015, in final form February 24, 2015

Colloidal particles grafted with single-stranded DNA (ssDNA) chains can self-assemble into a number of different crystalline structures, where hybridization of the ssDNA chains creates links between colloids stabilizing their structure. Depending on the geometry and the size of the particles, the grafting density of the ssDNA chains, and the length and choice of DNA sequences, a number of different crystalline structures can be fabricated. However, understanding how these factors contribute synergistically to the self-assembly process of DNA-functionalized nano- or micro-sized particles remains an intensive field of research. Moreover, the fabrication of long-range structures due to kinetic bottlenecks in the self-assembly are additional challenges. Here, we discuss the most recent advances from theory and experiment with particular focus put on recent simulation studies.

**Key words:** *DNA-functionalized nano-particles, self-assembly, experiment, theory, computer simulation*

**PACS:** *82.70.Dd, 87.14.gk, 81.16.Dn, 61.46.Df, 61.50.Ah, 75.75.Fk*

### 1. Introduction and overview

The miniaturization of technology demands new highly efficient methods to fabricate materials with desired optical, electronic and mechanical properties. To this end, the self-assembly of nano- and micron-sized particles functionalized with DNA strands has attracted much attention as a promising candidate for the formation of nano-crystals with long-range periodicity [1–3], as well as in applications such as sensing, imaging and therapeutics [4–12]. The role of DNA strands attached onto the surface of the particles is to stabilize soft non-compact crystalline structures by acting as links between the particles or as the intermediate matter. The structures depend on the size and geometry of the nano-particles (NPs), the surface density of DNA strands grafted onto the particles and parameters related to the DNA strands, such as the number of complementary bases which are available for hybridization [13]. Additionally, the occurrence of kinetically trapped structures during the self-assembly depends on thermodynamic conditions.

The idea of using DNA strands to create non-compact crystalline nano-structures was introduced by Alivisatos et al. [14] and Mirkin et al. [15], where gold (Au) NPs were used. These NPs are also referred to as polyvalent DNA Au NP conjugates [16] due to the large number of oligonucleotide chains grafted onto the NPs. Since then, much research is dedicated to understanding the self-assembly process of DNA-functionalized NPs and designing strategies that lead to specific crystalline structures. After almost two decades of intensive research in this field, a very good understanding has been achieved through a number of most interesting results. However, significant problems remain unsolved; for example, kinetic bottlenecks during the self-assembly process may result in the formation of unwanted crystalline, or

disordered structures. Moreover, synthesis of DNA-coated NPs in a controlled and accurate manner requires further improvement [17]. Therefore, the manufacturing of long-range ordered nano-structures required for many applications remains challenging. Additionally, bulk non-compact materials with a photonic band-gap in the range of visible wavelengths have not been achieved either [18].

Experimental, theoretical and computer simulation methods have contributed substantially to this area of research. While computer simulations offer some advantages related to the control of conditions over theory and experiment, limitations in system size and availability of reliable force fields underline the importance of a combined approach in studying the self-assembly of DNA-functionalized NPs. This review attempts to briefly present the key results in this research area with an emphasis put on the simulation side.

Experimental research and a range of applications of DNA-functionalized NPs have been previously discussed in a number of reviews [7–10, 19–25], while very little discussion has been reported on the recent progress of theoretical and simulation contribution to this area of research [26–29]. Part of the experimental discussion has focused on the synthesis, characterization and phase behavior of DNA-coated NPs assemblies [10, 17, 19–22, 24, 25], while others have concentrated on the possible applications of DNA-functionalized colloids [7–9].

Storhoff and Mirkin [25] have described the synthesis of DNA-programmed materials [30] referring to meso- and macroscopic organic structures from DNA at its infancy. Later, Macfarlane et al. have synopsized the key findings of their work suggesting fundamental design rules to predict the synthesis of distinct colloidal crystal structures with lattice parameters within the range 25–150 nm based on the independent adjustment of particle size, lattice periodicity and inter-particle distance [17, 23, 31]. For example, it was suggested [23, 31] that the overall hydrodynamic radius of a DNA NP dictates the assembly and packing behavior of the system, where the hydrodynamic radius is the size of the NP with the oligonucleotide components. NPs of equal hydrodynamic radius with self-complementary sequences self-assemble into fcc lattice, while CsCl or bcc lattices are obtained by using two different NPs with complementary DNA sequences [17], where the hydrodynamic radius can be measured by techniques, such as fast Brownian motion analysis [32]. It has been found that DNA NPs with equal hydrodynamic radii will maximize the number of hybridization events between neighboring colloids. Additionally, the size ratio (expressed through the ratio of the hydrodynamic radii) and the DNA linker ratio (the ratio of the number of DNA linkers) between two NPs control the thermodynamically favored crystal structure [23]. In particular, the size ratio determines the packing of particles in the crystal and its stability, while the linker ratio determines the stability of the crystal. Therefore, two systems with the same size and linker ratio exhibit the same “thermodynamic product” [17, 23]. The final crystal structure is the one that maximizes the DNA sequence-specific hybridization interactions. It has been also shown that similar structures can be produced by varying the rate at which individual DNA linkers dehybridize and subsequently hybridize [23]. These conclusions have been reproduced by using a simple model based on the assumption that DNA sticky ends should physically contact each other to hybridize and that any sticky ends coming into contact will eventually form a DNA duplex. Hence, this simple model can be used as a tool to inform the self-assembly of DNA-functionalized spherical NPs [23]. The work of Macfarlane et al. [17, 23, 31] highlights the key experimental achievements and conclusions regarding the self-assembly of spherical colloids via DNA-mediated interactions [17, 23].

Conjugation and characterization methods, three representative self-assembly strategies of the self-assembly of DNA NPs into super-lattices [24], and design principles for plasmonic nano-structures [10, 33–35] have been recently discussed. For example, how DNA has been used to build finite-number assemblies (plasmonic molecules), molecularly driven plasmonic switches [36], regularly spaced NP chains (plasmonic polymers), and extended two- (2D) and three-dimensional (3D) ordered arrays (plasmonic crystals) [10, 37], as well as DNA patchy particles [38] and oligonucleotide capsules [39], and the formation and stability of surface-tethered DNA gold-dendron NPs [40] have been discussed. Some work has dealt with the plasmid-templated shape control of condensed DNA block copolymer NPs [41]. Of particular interest has also been the integration of self-assembly with top-down lithography [21] for nano-patterning of materials onto substrates [42].

Geerts et al. [20] have reviewed various aspects of DNA-functionalized NPs self-assembly, such as the synthesis of DNA NPs nano-complexes, their physical properties and a range of applications for nano- and micron-sized colloids either in two- or three-strand systems. At the same time, in two-strand systems,

the DNA strands belonging to different NPs hybridize directly to each other, in three-strand systems a third DNA linker is required for binding the DNA strands belonging to different NPs. The effect of the number of base pair matches, length, DNA grafting density on the colloidal surface, ionic strength of the surrounding medium and effects of pH and solvent polarity, etc., are parameters discussed in this work. In particular, understanding and controlling DNA-mediated interactions between colloidal particles is a key to the self-assembly process. A number of factors contributing to these interactions have been investigated by experiments, theoretical studies and computer simulations designed to investigate interactions and aggregation/melting behavior of DNA-functionalized NPs [28]. Moreover, the clustering of DNA-functionalized colloids that occurs during the self-assembly shares similarities with percolation phenomena [43]. Geerts et al. [20] have also discussed 1D, 2D and 3D assemblies of DNA-functionalized colloids, where for the 3D assemblies an account of micron- and nano-sized NPs is given. Additionally, a discussion on the broad range of applications of such systems is provided focusing on applications such as the detection of small molecules with DNA sequences (bio-recognition, e.g., within the cell), or DNA/RNA delivery into cells [20].

The self-assembly of DNA-functionalized colloids has been interesting in a number of different contexts apart from the self-assembly. For example, recent advances in the synthesis of bio-molecule NP/nanorod hybrid systems applications in the generation of 2D and 3D ordered structures in solutions and on surfaces have been a large area of research [22]. The potential use of bacteria as a novel biotechnology to facilitate the production of NPs is also an important application, while emphasis has been also put on bio-molecule-NP assemblies for bio-analytical applications and for the fabrication of bio-electronic devices [22]. Examples of such applications are sensors, bio-molecule-functionalized magnetic particles, and bio-molecule-based nano-circuitry and viral templates [22]. Also, composite assemblies of nucleic acids, proteins and NPs have been discussed in the literature [22], as well as the protection and promotion of UV radiation-induced liposome leakage via DNA-directed assembly with gold (Au) NPs [44, 45].

Heuer et al. [7] highlighted the importance of Au functionalized conjugates for biomedical applications (e.g., biological sensing [46]) while suggesting a copper-free click chemistry for the programmed ligation of DNA-functionalized Au-NP [47]. The focus has been on the invention and applications of “nano-flares” [48–50], which carry reporter duplexes being released after binding. This signal provides the ability to detect specific endo-cellular targets such as mRNAs, microRNAs, or ions and small molecules in real time. Their properties, stability, cellular uptake and cytotoxicity have been the main focus for such systems. However, the design of many more highly multiplexed systems with improved targeting properties are to be expected in the near future. Sokolova et al. [9] discussed the transfection of cell with DNA NPs and methods for gene transfer into living cells, while Rosi et al. [8, 11] focused on the use of these nano-structures in bio-diagnostics, for example electrical and electrochemical detection, magnetic relaxation detection, and nano-wire and nano-tube-based detection. Another application relates to the colorimetric recognition of DNA intercalators with unmodified Au-NPs [51].

Molecular dynamics simulations and theoretical methods related to the self-assembly of DNA-functionalized NPs have been briefly discussed previously [26, 27, 52]. A recent review has summarized the main theoretical and simulation models in the context of recent experimental progress, highlighting the advantages and disadvantages of these models and key findings [29]. Moreover, the crystalline structures obtained so far by experiment have been summarized [29]. Despite the above discussion, a complete presentation of the theoretical and simulation contribution to the field is still lacking. This review intends to fill this gap and aims at presenting key experimental findings and an overview of theoretical and simulation studies that have contributed fundamentally to understanding the self-assembly of DNA-functionalized NPs.

## 2. Experiments

### 2.1. Synthesis and experimental methodology

A number of DNA-functionalized NPs-based structures can be formed by tuning independently the NPs size, shape, and composition. However, a general strategy for the synthesis of DNA-functionalized NPs has been discussed only recently [53], where also NPs with high-density shells of nucleic acids can

be built. Specific coating technology on the NP surface has been implemented in order to realize this general synthetic strategy of DNA-based self-assembly. The creation of heterogeneous NP super-lattices is based on carboxylic-based conjugation [54]. These heterogeneous materials have novel optical and field-responsive properties, which are achieved by a careful selection of NP characteristics, such as size, shape, and the number of DNA strands per particle and DNA flexibility [17, 54]. An important advance in the synthesis of DNA-coated NPs is the synthesis of solid colloids with surface-mobile DNA linkers [55]. In this case, the DNA linkers are fully mobile on the surface of the NP, and the temperature range for equilibrium self-assembly is much broader than in the case of immobile linkers. By increasing the temperature window for melting, a better control of the self-assembly process can be achieved, because fast crystallization leading to kinetically trapped nano-structures can possibly be avoided. Moreover, linkers accumulate at the NPs below the melting temperature, thus increasing the number of hybridization events and the stability of the final assembly structure [55]. A recent computer simulation study has drawn similar conclusions [56].

Although initially the self-assembly was based on Au NPs, self-assembly based on silver NPs conjugates by using triple cyclic disulfide moieties [57] or metal oxide NPs [58] has been also reported. DNA-induced size-selective separation of mixtures of Au-NPs is also possible [59] by using the co-operative binding properties of DNA-functionalized NPs. This is based on the fact that the melting temperature of the NPs aggregates depends on the size of the NPs [60]. Then, a combination of sedimentation and centrifugation techniques can be used to separate larger NPs from smaller ones [59]. This method of separation of NPs according to their size has also been demonstrated in the case of a ternary mixture [59]. Controlled structural evolution of large silver NPs and their DNA-mediated bimetallic reversible assemblies [61] has been recently studied by Kim et al. [62], as well as the synthesis and reversible assembly of DNA Au-NP cluster conjugates [63].

It has been recently shown that in binary mixtures of sub-micron colloids, certain crystals can be obtained from parent crystals by diffusionless transformations, analogous to the Martensitic transformation of iron [64]. This also provides a possibility of accessing certain structures by these parent crystals, which otherwise would be kinetically unaccessible, though this structure has a lower energy. An example of this approach is the formation of a CuAu-I structure from a CsCl crystal structure [64]. This work underlines the fact that structural transformation of atomic solids may also occur in DNA-linked NPs. An exciting feature of DNA NP assembly structures is that the NP crystals form reversibly during heating and cooling cycles. For example, the bcc lattice structure is temperature tunable and non-compact with particles occupying only a small fraction of the volume of the unit cell [65, 66]. The compression properties of DNA NPs assemblies have been studied by measuring their response to the applied osmotic pressure showing that lattices based on these materials are super-compressible and capable of transforming between different structures [67]. This explains the capability of these systems of transforming between different structures. The lattices of nano-particles interconnected with DNA, exhibit an isotropic transformation under compression with a remarkably strong decrease of the lattice constant, up to a factor of about 1.8, corresponding to more than 80% of the volume reduction [67]. The force field extracted from experimental data can be well described by a theoretical model that takes into account the confinement of DNA chains in the interstitial regions. It has been shown that compression properties of these systems can be tuned via DNA molecular design [67]. Moreover, the structural plasticity of bio-molecules and the reversibility of their interactions can also be used to make nano-structures that are dynamic, reconfigurable, and responsive. The inter-particle distances in the super-lattices and clusters can be modified, while preserving structural integrity by adding molecular stimuli (simple DNA strands) after the self-assembly processes have been completed. Both systems were found to switch between two distinct rigid states, but a transition to a flexible state configuration within a super-lattice has shown a significant hysteresis [68].

The crystal growth depends on the length of DNA linker, the solution temperature, and the self-complementarity of DNA strands and can be compared to the case where non-self-complementary DNA linker strands are used [69]. A three-step process for crystal growth has been suggested, i.e., an initial “random binding”, resulting in disorder Au-NP aggregates, a localized reorganization, and a subsequent growth of crystalline domain size, where the resulting crystals are well-ordered at all subsequent stages of growth [69]. A stepwise growth process to systematically study and control the evolution of a bcc crystalline thin-film of DNA-functionalized NPs on a complementary DNA substrate has been recently pre-

sented [70]. This crystal growth on a substrate has been examined as a function of the temperature, the number of layers, as well as the substrate-particle bonding interactions. In this case, the interfacial energy between various crystal planes and the substrate were tuned by the DNA interactions controlling the crystal orientation and size in a stepwise fashion using chemically programmable attractive forces. This is a unique approach, since the prior studies involving super-lattice assembly typically relied on repulsive interactions between particles to dictate the structure, and those that relied on attractive forces (e.g. ionic systems) still maintained repulsive particle-substrate interactions [70]. Indeed, to date, 17 unique symmetries have been realized and over 100 unique crystal structures have been synthesized, all of which conform to a key hypothesis: the obtained assembly structures maximize the total number of hybridized DNA interconnects between particles [70].

The number of possible lattices for synthetically programmable NP super-lattices can be increased by using a hollow 3D spacer approach [71]. In this approach, some NPs within a binary lattice can be replaced with “spacer” entities that are designed in such a way as to replace the behavior of the missing NPs. For example, the NPs of one type are omitted by the structure without affecting the positions of the other NPs. In this way, super-lattices with five distinct symmetries have been created, including the one that has never been observed before in any crystalline material [71], while the nano-meter precision in lattice parameter tunability has been maintained [71]. Although hexagonally close-packed arrays of NPs are quite commonly made by different assembly strategies, simple hexagonal lattices of NPs have been more difficult to create, because close-packed structures are often energetically more favorable. Furthermore, a graphite arrangement of spherical NPs has never been made by any assembly method. However, by applying the 3D spacer approach to the  $AB_2$  lattice, both of these lattices are easily synthesized and exhibit a crystalline order with micro-meter-sized domains [71]. Hollow triangular gold-silver alloy nano-boxes have been also reported [72], a process which is reversible upon heating with sharp melting transitions, which has been monitored at wavelengths throughout the visible and near-IR.

## 2.2. Phase behavior and influence of various parameters

An elegant way to regulate the range and magnitude of forces between pairs of different particles is based on the control of the specific DNA linkages between colloidal particles self-assembly through the combination with polymer brushes [73]. Such self-assembly has been found to be a reversible process. The key of reversibility is not to allow the particles to be very close, where van der Waals forces become important. This is why the presence of adsorbed polymers is required [73]. In fact, DNA-functionalized Au NPs in macromolecularly crowded polymer solutions have been recently reported [74].

The inter-particle distance of fcc structures can be tuned by increasing the DNA linker length or the total DNA length [75]. Structures containing less than 0.52% of inorganic material have been synthesized, enabling the tuning of the unit cell lattice parameters within a large range of values [75]. Moreover, the stability of the structures depends on the sequence of the DNA bases [76, 77]. Namely, different DNA sequences will guide the self-assembly of these NPs into different structures [78]. In binary mixtures, the degree of binding between complementary beads depends also on the number of matching pairs and the ionic strength of the solution [79]. A large variety of colloidal structures, such as chains of alternating large and small particles for a large range of particle number ratios and volume fractions have been investigated [79]. Also, the plasmon coupling strength depends strongly on the length of the DNA connecting Au-NPs [80]. The choice of the DNA linking molecules and the absence or presence of a non-bonding single-base flexor can be adjusted, so that Au NPs assemble into micro-meter-sized fcc or bcc crystal structures. These results demonstrate that a single-component system can be directed to form different structures [78]. Moreover, particles with a poly-dispersity of 20% do not form well-defined crystalline assemblies. Crystalline structures usually require a poly-dispersity of NPs below 10% [78].

For 3D hybridization with polyvalent DNA Au NP conjugates [16], it has been found that there is a minimum number of base pairings necessary to stabilize DNA Au NP aggregates as a function of salt concentration for particles between 15 and 150 nm in diameter. Sequences containing a single base pair interaction are capable of effecting hybridization between 150 nm DNA Au NPs. While traditional DNA hybridization involves two strands interacting in one dimension (1D, Z), hybridization in the context of an aggregate of polyvalent DNA Au NP conjugates occurs in 3D making NP assembly possible with three or fewer base pairings per DNA strand. These studies enable the comparison of the stability of duplex

DNA free in solution and bound to the NP surface. It has been found that 4–8, 6–19, or 8–33 additional DNA bases must be added to free duplex DNA to achieve melting temperatures equivalent to hybridized systems formed from 15, 60, or 150 nm DNA Au NPs, respectively [16]. In addition, the equilibrium binding constant ( $K_{\text{eq}}$ ) for 15 nm DNA Au NPs (three base pairs) is three orders of magnitude higher than the  $K_{\text{eq}}$  of the corresponding NP free system [16].

Xiong et al. [81, 82] provided the first experimental phase diagram of the NPs assembled by DNA linkers in terms of nominal DNA linker/Au-NP ratio  $r$  and volume fraction  $\eta$ , where the boundary between disordered and bcc structures has been determined. The formation of a crystalline bcc phase was observed for a limited range of linker lengths, while the number of linkers per particle controlled the onset of system crystallization. The effect of linkage defects on the crystalline structure was also examined. Note that these results were corroborated later by computer simulations [83].

Although a broad range of different non-compact structures has been created over the last years [84], a single-component NP assembly of a diamond structure has not been reported. By a delicate tuning of the particle interactions, binary diamond-like crystalline structures have been fabricated [84] though. For example, NaTl-type non-compact structures have been reported, using surface-modified Q $\beta$  phage capsid particles and Au-NPs of similar radii. This structure has an inorganic component and an organic virus-like protein NP interpenetrating diamond lattices. This is an example where particles of different chemical nature can be combined after a proper surface processing, without phase separation taking place. However, protein-based structures had been discussed already before [85], in addition to the inorganic NPs [86]. NP-DNA conjugates bearing a specific number of short DNA strands by enzymatic manipulation of NP-bound DNA have been also reported [87], as well as the self-assembly of icosahedral virus particles organized by attached oligo-nucleotides [88], and binary heterogeneous super-lattices assembled from quantum dots and Au-NPs with DNA [89], or assembling colloidal clusters using crystalline templates and reprogrammable DNA interactions [90].

### 2.3. Micron-sized nano-particles

Micron-sized latex particles with single-stranded DNA grafted to the surface have been used as a model system to study DNA mediated interactions [91]. The presence of DNA strands allows for the tuning of the interactions between NPs by combining hybridizing linker DNA with non-hybridizing neutral DNA, which leads to a gradual change of the assembly rate. The effect of linker/neutral DNA ratios on particle assembly kinetics and aggregate morphology has been experimentally investigated for a range of ionic strengths. The conditions for controlling various assembly morphologies have been identified, and the involved attractive and repulsive interactions have been described and explained for the proposed approach, also accounting for further theoretical considerations [91].

Kim et al. [92, 93] have reported on the first DNA-mediated micrometer sized colloidal crystals by using polystyrene particles, discussing preparation strategies of these colloids in order to obtain such crystals. Thermodynamic properties of the self-assembly of these crystals are also predicted through a simple thermodynamic model. Possible ways of obtaining more ordered structures by studying the growth kinetics and phase behavior of the self-assembly of DNA-functionalized colloids have been also considered [93]. Various aspects of the selective, controllable, and reversible aggregation of polystyrene Latex micro-spheres via DNA hybridization have been discussed [94]. These systems were found to have interesting kinetics and non-exponential binding behavior [95].

The first direct measurements of DNA-induced interactions between a pair of micron-sized polymer colloids have been conducted by Biancaniello et al. [96] by using an optical tweezer method. These results can be modelled using standard statistical mechanics methods. It has been shown that micron-sized spherical colloids have binding dynamics of a power-law in annealing and crystallization processes. Additionally, the phase behavior of DNA-mediated micro-sphere suspensions was determined as a function of salt and oligonucleotide concentration [97]. In this case, fluid phases, aggregate phases, or mixed fluid phases with aggregates have been observed, while increasing salt or hybridizing events favors the formation of aggregates. Forces of interaction between DNA-grafted colloids via optical tweezer measurements have been also reported elsewhere [98], in quantitative agreement with a proposed theoretical model [99]. The specific interaction of DNA-functionalized polymer colloids by using DNA linkers in solution has

been also reported [100]. Based on such measurements, a Monte Carlo (MC) scheme to describe colloidal crystallization has been implemented [101, 102].

Switchable self-protected attractions in DNA-functionalized spherical colloids are also very interesting [103]. For example, single-stranded DNA can fold creating secondary structures, such as loops and hairpins [104–107], which influence the self-assembly. For micron-sized particles, these structures provide a control over inter-particle binding strength and association kinetics. By heating and cooling the system, one can mediate these effects. Such topological interactions may lead to new materials and phenomena, like particles strung on necklaces, confined motions on designed contours and surfaces, or even colloidal arrangement in the shape of “Olympic gels” [104]. Also, polyvalent nucleic acid nano-structures (PNANs), which are composed of only cross-linked and oriented nucleic acids, are of great interest. Apart from the self-assembly properties, these particles are capable of effecting high cellular uptake and gene regulation without the need of a cationic polymer co-carrier [108].

## 2.4. Anisotropic DNA-functionalized nanoparticles

Some structures cannot be fabricated by using only spherical colloids in all dimensionalities. Hence, directional bonding interactions which can be tuned by the different geometry of the NP have been used for a better control over the directed self-assembly of such DNA NPs. One advantage of using particle anisotropy is the fact that a greater surface contact favors a higher number of hybridizations. Moreover, the effective local concentration of terminal DNA nucleotides that mediates hybridization increases, while conformational stresses imposed on nano-particle-bound ligands participating in interactions between curved surfaces might be smaller [17, 109]. DNA NPs with core particles of different shape have been synthesized in a way to study the effect of the core-core particle interactions, affecting super-lattice dimensionality, crystallographic symmetry and phase behavior [109, 110].

An example of 1D structures is the self-assembly of nano-rods [111], where again the most stable structure is the one that maximizes hybridization events between DNA sticky ends [23]. Moreover, for octahedron NPs, one might obtain fcc or bcc structures depending on the length of the DNA strands. However, previous work [109, 110] has obtained self-assembly aggregates rather than real long-range crystal structures indicating the difficulty in obtaining long-range crystalline structures. Recently, the use of DNA-driven assembled phospholipid nano-discs as a scaffold for Au-NP patterning has been discussed [112]. A facile and efficient preparation of anisotropic DNA-functionalized Au NPs and their assembly has been reported recently [113]. This one-step solution-based method has been used to prepare anisotropic DNA-functionalized Au-NPs with 96% yield and with high DNA density. Well-defined nano-assemblies using Au NPs having a specific number of DNA strands have been also discussed [114]. Periodic square-like Au NP arrays templated by self-assembled 2D DNA nano-grids on a surface have been also reported in the literature [115], as well as multiple-nano-component arrays by 2D DNA scaffolding [116]. Triangular gold nano-prisms [117] in the presence of attractive depletion forces and repulsive electrostatic forces assemble into equilibrium 1D lamellar crystals in solution with inter-particle spacings greater than four times the thickness of the nano-prisms [118]. Experimental and theoretical studies reveal that the anomalously large spacings of the lamellar morphologies are due to the balance between depletion and electrostatic interactions [118].

DNA-directed assembly of asymmetric nano-clusters using Janus NPs has been also investigated [119, 120]. Curvature effects in DNA Au-NP conjugates are notably important, due to the asymmetry of the NP [121, 122]. Particle curvature also plays an important role in controlling the DNA surface density [122]. Based on such an approach, there is a method to predict DNA packing on non-spherical particles. An example of usage has been provided for Au nano-rods [122]. Linear micro-structures in DNA nano-rod self-assembly have been reported recently [123]. Fibers, tubules, and ribbons are typical 1D nano-structures that require anisotropic interactions that also emerge from the geometry of the NP, which affects the underlying inter-particle interactions during the structure formation. For systems of DNA-functionalized nano-rods, the resulting structures are 1D ladder-like meso-scale ribbons with a side-by-side rod arrangement. Moreover, the DNA can bind reversibly, facilitating in this way the formation of hierarchical assemblies with time. Linear structures of alternating rods and spheres have been also obtained, implying the generic applicability of the mechanism for nano-scale objects interacting via flexible multiple linkers [123].

## 2.5. Self-assembly in one- and two-dimensional geometries

DNA-based self-assembly of NPs has been discussed in the context of planar or other geometries, as, for example, in the case of DNA-mediated 2D colloidal crystallization above different attractive surfaces [124]. Cheng et al. [125] reported the first DNA-based strategy for mono-layered free-standing NP super-lattices or very thin films. In this case, discrete free-standing super-lattice sheets can be obtained without the requirement of Watson Crick's specific binding in which inter-particle spacing occurs within the structure, leading to the formation of plasmonic and mechanical properties that can be rationally tuned by adjusting the DNA length [126]. Moreover, thin standing films based on DNA-coated colloids with double-stranded DNA have been reported [127]. Such colloids can self-assemble into unique crystalline mono-layers, suspended at a distance of several colloidal diameters above a weakly adsorbing substrate, without a dependence on DNA hybridization. The advantage of such systems is that they can be prepared in one location and then be used in a different application somewhere else. This may be a way for the assembly of multi-component, layered colloidal crystals [127]. Moreover, responsive multi-domain free-standing films of spherical Au-NPs assembled by DNA-directed layer-by-layer approach have been also studied recently [128]. Large-area spatially ordered arrays of Au-NP crystals directed by lithographically confined DNA origami have been also synthesized [129] and 5 nm size Au-NPs arranged into long-range ordered 2D arrays onto lithographically patterned substrates [129]. Additionally, the first DNA-mediated formation of supra-molecular mono- and multi-layered NP structures has been presented [130], as well as DNA and DNAzyme-mediated 2D colloidal assembly [131].

## 3. Computer simulations

Various simulation models for DNA chains have been contrived over the last years [132–143]. As it usually happens with these models, they aim at reproducing only the properties of interest of the system. Due to the large system sizes and time scales required in the study of DNA or DNA-coated NPs, mainly coarse-grained models are capable of describing relevant phenomena or bespoke theoretical models, such as the self-assembly of DNA-functionalized NPs.

### 3.1. Coarse-grained models

Starr and Sciortino [142] have proposed a simple model for the study of the self-assembly of DNA-functionalized NPs (figure 1). This model has been used for short DNA strands (six to twelve bases) and specific DNA sequences. The effect of several parameters has been explored, for example, the number of bases per strand, the number of linking bases and the number of spacer bases on the stability of crystal states, as well as the effect of using a single linking NP type versus a binary linking system. Additionally, the free energy, entropy, and melting point for bcc and fcc lattices have been explicitly calculated. While binary systems preferably form bcc lattices, melts of single NP type with chains of self-complementary basis form the most stable fcc crystals. A way to maximize a crystal stability based on the heat of fusion between crystal and amorphous phases growth has been discussed [144]. The stability of bcc and fcc crystals formed by DNA-linked NPs has been further investigated [145] as a function of the number of attached strands to the NP surface, the size of the NP core, and the rigidity of the strand attachment. It has been found for this model that relaxing the condition of kinetically immobile strands on the surface of the particles, a slight increase or decrease in the melting temperature occurs. Larger changes to the melting temperature result from increasing the number of strands, which increases the melting temperature, or by increasing the core NP diameter, which decreases the melting temperature [143]. A quantitative description of the melting temperature has been provided by the model of Starr and Sciortino [142–144]. This model has been fully investigated and used in the study of self-assembly process [146, 147]. In these studies, a phase diagram for the NPs as a function of temperature and NPs density has been provided.

Furthermore, the effective potential between DNA-functionalized NPs can be obtained enabling the comparison of the phase diagram of effective particles with the phase diagram of the NPs based on the full coarse-grained description. Various grafting geometries have been considered in studying the self-assembly, such as triangular planar, tetrahedral, square-based pyramid, triangle-based bipyramid, and

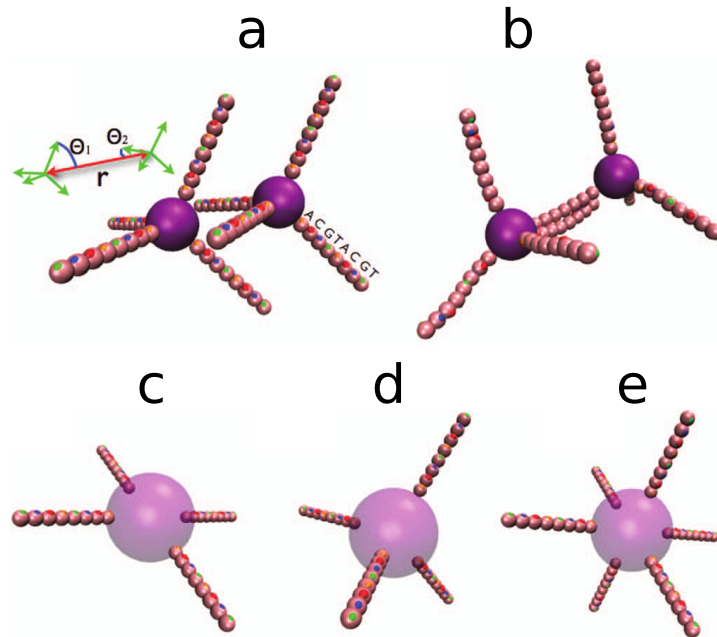


**Figure 1.** (Color online) Schematic representation of the model of Starr and Sciortino [142]. This model considers only a specific DNA sequence (specified in panel a) which leads to the hybridization shown in panel (b). This model can assume different DNA lengths, NPs sizes and grafting geometries (c)–(e). The effective potential between two NPs modelled in this way depends on the angles  $\theta_1$  and  $\theta_2$ , and the distance  $r$  between the NPs. Further details on how to calculate the effective potential can be found in [143]. Figure adapted from [143] after permission.

octahedral geometries [147]. These NPs have short DNA strands with imposed rigidity and complementary DNA sequences resembling interactions between patchy colloids. For all these geometries, but the octahedral one, there has been found a phase behavior analogous to gas-liquid transition. For the octahedral geometry, various crystal structures of similar symmetry occur, depending on the chemical potential (density) of the system. Then, interpenetrating networks of DNA-functionalized NPs occur [147]. In the following study [148], a two-step crystallization of DNA-functionalized NPs has been discussed, where the narrow temperature range that the self-assembly takes place is described through a two-step process, mediated by a highly connected amorphous intermediate. Moreover, at lower temperatures, the system is kinetically trapped hindering crystallization [148]. By using a standard cluster analysis and relevant order parameters based on spherical harmonics, the structures and their degree of crystallinity were resolved. The relaxation and crystallization times of such systems have been also studied [148]. Different amorphous networked phases induced by multiple liquid-liquid critical points providing a phase diagram of the temperature versus density have been identified [149], based on effective NPs. This effective potential has been carefully revised in the following work [143]. Different structure factors can describe the interpenetrating networks as the density of the NPs increases [149].

The equilibrium clustering dynamics and the self-assembly kinetics can be described on the basis of the Flory-Stockmayer theory [150–152] finding good agreement among theory and results obtained from the coarse-grained model. Considering only two- and three-fold NPs in order to facilitate the branching between two-fold DNA NPs, percolation and phase separation at low density have been studied [152]. Furthermore, the kinetics of the self-assembly are investigated in terms of the bond formation rate as a function of temperature and time [152]. It has been found that these processes follow an Arrhenius behavior, where the self-assembly is described by two “reaction” constants. The model of Starr and Sciortino [142] has been also used to study the effects of bidispersity in DNA strand length [153] and effects of DNA strand sequence and composition [153, 154]. Moreover, NP dimers linked by DNA can be used as the building blocks of a multi-scale, hierarchical assembly, especially when the size of the NPs is similar [155]. The structure of NP dimers through a combination of scattering experiments and molecular sim-

ulations has been recently investigated [155]. It has been found that the inter-particle separation within the dimer is mainly controlled by the number of hybridized DNA strands, their length and the curvature of the particle, as well as the excluded volume effects. Without any free parameters, the increase of dimer separation with increasing temperature can be interpreted as a result of the change in the number of connecting DNA [155]. Recently, it has been shown that tetravalent DNA nano-stars never crystallize, but they form a fully bonded equilibrium gel [156]. The phase diagram of these organic complexes has been also discussed [157].

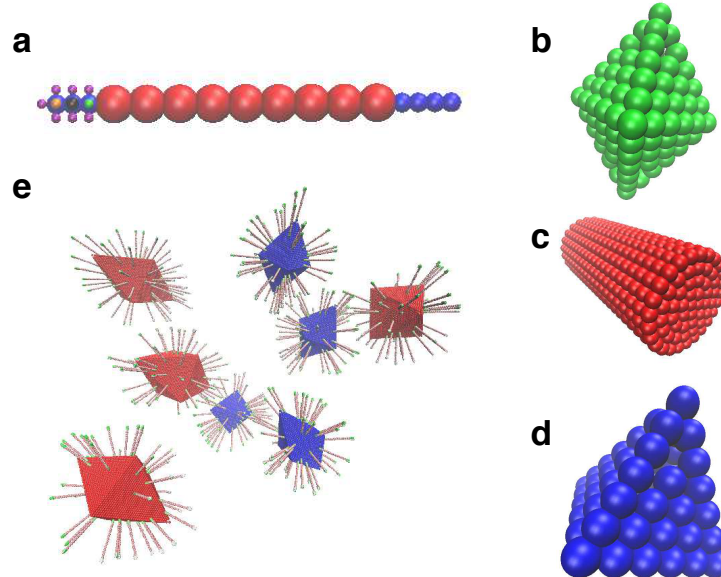


**Figure 2.** (Color online) Schematic representation of the model by Li et al. [161], as adapted from the original model of Knorowski et al. [83]. In panel (a) we present a typical DNA chain. Blue beads indicate flexible ssDNA, red beads dsDNA, while green, black, and orange beads represent DNA bases. The magenta flanking beads have been originally used in [83] to prevent double bonding, in this way overcoming a drawback of the model of Starr and Sciortino [142]. Li et al. have used spherical particles for their simulations, but different geometries can be used as those in panels (b), (c), and (d). In panel (e), we present an initial configuration for MD or MC simulation of DNA-functionalized octahedra based on the model of Li et al. [161].

A model that is closer to the experimental expectations has been proposed by Knorowski et al. [83, 158, 159] and has been amended by Li et al. [160] to match the experimental energy and length scales (figure 2). Apart from a number of different structures and the very good prediction of the experimental phase diagram as a function of the volume fraction, temperature, and grafting density, this model is capable of describing the dynamics and thermodynamics of the self-assembly process. The D-bcc crystalline phase also exists in their phase diagram. In this case, two different types of DNA-functionalized NPs occupy the positions of a bcc lattice, but the type of particles does not have the same pattern across the crystalline structure. This effect has been previously overlooked. Moreover, a CsCl-bcc structure is a part of the phase diagram, while the exact boundary with disordered structures has been determined, providing the universal dynamics of the crystallization process [83]. This model has in many different aspects overcome the problems of the modelling approach of [142], such as the possibility of a strand to bind to more than one complementary DNA strands. Recently, this model has been used to study in more detail the crystallization dynamics, such as gelation, nucleation, and topological defects [159]. The formation of crystals involves various dynamic stages of the system, starting from a liquid mixture to the formation of a gel. Then, the formation of a crystal containing defects takes place, and finally an equilibrium structure forms [159]. For these stages, the dynamics of the process have been discussed in detail [159]. Li et al. [160] have actually used this model [83] to study the phase diagrams as a function of size ratio and DNA coverage ratio as is done in experiment [31]. The authors confirmed fully the experimental observations [23, 31].

In a follow-up study [161], it was found that the thermally active hybridization drives the crystallization of DNA-functionalized NPs. By using Molecular Dynamics (MD) simulations, the dynamic aspects of the assembly process were analyzed and the key ingredients to a successful assembly of NP super-lattices have been identified. The conclusions of the simulation model are scalable, being able to reproduce the experimental observations, which have proposed various structures [161]. Moreover, the optimum percentage of DNA hybridization events has been determined for different binary systems, being able to propose suitable linker sequences for future nano-material design [161]. Recently, this model, in combination with experiments, has been used to investigate the DNA-mediated NP crystallization into Wulff polyhedra, where the use of DNA-functionalized NPs offer a higher control over the growth process of the crystals [162].

The pair interactions between DNA-functionalized colloids have been the main topic in the field [137], and among other methods, MC simulations considering NPs with short and stiff DNA chains have been employed [163]. Such interactions have been initially measured for planar surfaces corresponding to large NPs. Based on simulation results, analytical expressions for the interactions can be obtained, claiming that this is a valid description for a range of NPs from the nano- to the micro-meter scales, as well as for a large range of grafting densities. Moreover, important contributions to the repulsive and attractive terms of the free energy are coming from purely entropic effects of the discrete tethered sticky ends. Such entropic contributions compare well with the hybridization free energy of a free pair of sticky ends in solutions. Stable gas-liquid separation only occurs for NPs with radii of a few tens of nanometers, suggesting different crystallization routes for nano- and micron-sized NPs [163]. Statistical anisotropy on the distribution of sticky ends on the NPs' surface leads to a large variation of the binding strength. This may weaken the reliability of tests based on the detection of DNA targets in diagnostics. These results provide a general background for the systems with tethered binding groups [164], as for example in the areas of supra-molecular chemistry or ligand/receptor mediated bio-recognition [163]. Based on this MC coarse-grained model, a new strategy to improve the self-assembly properties of DNA-functionalized colloids has been proposed [165]. The narrow crystallization temperature window is due to the sensitivity of DNA-mediated interactions to temperature and other physical control parameters. By exploiting the competition between DNA linkages with different nucleotide sequences, this temperature window can become larger. Thus, the temperature dependence of the self-assembly process has been decreased offering a control over a larger temperature range. Such an approach is also applicable in a realistic situation, where the control is due to a combinatorial entropy gain, which stems from the large number of binding partners for each DNA strand. Experimental work has suggested particular DNA sequences that are capable of reproducing those effects [165].

The narrowness of the temperature has been also addressed in another study by Uberti et al. [166], since this narrow temperature window from dilute systems to aggregates reduces considerably the capability of obtaining defectless crystal structures, thus restricting the number of possible crystal structures. A design of DNA-coated colloids which crystallize on cooling and melt on further cooling has been proposed [166]. Although this is a mere theoretical model-assumption, it has been argued that realistic situations that can follow such a phase behavior do exist. While the results presented refer to binary systems, these concepts also apply in multi-component systems, opening the way towards the design of truly complex self-assembling structures based on spherical colloids [166]. The implications of these results have been commented by Gang [167]. Latest techniques exploit the narrow temperature window though, in order to construct amorphous materials with specific morphology and local separation between multiple components. In this regard, strategies to direct the gelation of two-component colloidal mixtures by sequentially activating selective interactions have been proposed [168]. Changes in the structure can be investigated via MD simulations and experimental methods. This approach in studying the multi-step kinetics of the self-assembly process can be extended to the assemblies of multi-component meso-porous materials with possible applications in hybrid photovoltaics, photonics, and drug delivery [168].

MC simulations combined with histogram re-weighting techniques have been applied in order to construct the phase diagram of DNA-functionalized NPs based on a coarse-grained model [169]. This model can predict the phase separation between a dilute vapor-like phase and a dense phase where NPs are a part of a liquid-like network based on DNA links. In this case, there is a non-monotonous dependence of the coexistence pressure on the temperature, namely the reduced hybridization free energy [169]. This behavior may be attributed to the crossover between two distinct regimes. Namely, the hybridization-

free-energy driven regime and an entropy-driven regime. In the former case, there is a “normal” vapor-liquid equilibrium, where the system gains free energy but loses entropy. In the entropy-driven regime, an increase in entropy occurs due to the rearrangement of sticky-end bonds in the liquid phase. The main conclusion of this work is that the system undergoes a phase separation if the number of DNA-chains per NP is larger than two. As the number of chains increase, the coexistence region increases considerably [169]. In another MC study [170], the phase behavior of colloids coated with long, flexible DNA chains, which can also be achieved experimentally [171], has been investigated. In this case, when the number of DNA strands per NP decreases below a critical value, the triple point disappears. Also, the condensed phase coexisting with the vapor remains a liquid. This result may explain the reason why NPs with small DNA coverage cannot crystallize in dilute solutions highlighting in this way the discrete nature of DNA binding [170].

In another coarse-grained approach realized in a MC scheme, a simplified model was proposed, based on experimental data, which can describe the phase behavior for DNA-coated colloids [172]. These results have indicated that the assumption of pair-wise additivity of DNA-mediated interactions lead to substantial errors in the estimation of the free energy of the crystal phase. While these simulations correctly predict the experimentally obtained crystal structures, despite uncertainties in the estimates of contour and persistence lengths of ssDNA chains, they also provide a good estimate of the melting temperature [172]. Hence, further, more accurate experimental results are required in order to construct a more accurate coarse-grained approach [172].

The effect of linear shear force on the self-assembly of DNA-functionalized colloids in two dimensions has been also investigated [173]. A better sampling of the phase space is possible in binary systems. From the constructed phase diagram, a linear dependence of the minimum DNA force necessary for the line formation on the dimensionless shear rate was found. By employing a force analysis on the obtained structures, a linear orientation perpendicular to the axis of the elongations component of the shear was found, which is the orientation that enables the DNA attraction to resist to shear [173]. The effect of internal viscoelastic modes on the Brownian motion of a 1-DNA coated colloid is yet another topic of recent research [174].

Spherical NPs of 1 mm colloids bridged by DNA with 32mm contour length have been studied in a mixture of two types of particles with grafted double-stranded 1-DNA with short complementary single stranded overhangs as free binding ends. Confocal microscopy identified the formation of stable size-limited clusters in which the two types of particles are in contact. The simulations suggest that entropic exclusion of the bridging DNA from space between the nearby particle surfaces hinders the formation of crystals in millimeter-sized NPs [175].

### 3.2. Further models, theoretical, and numerical approaches

Specific attraction between NPs can be induced by DNA bridging creating a large number of periodic structures. Although the thermodynamics of DNA-functionalized NPs in solution is well-understood, perfectly suitable coarse-grained models are still challenging. This difficulty has hindered the design of complex temperature, sequence and time-dependent interactions required to describe, for example, materials with highly complex or multi-component micro-structures or the ability to reconfigure or self-replicate. A recent study [176] has provided high resolution measurements of DNA-mediated interactions in polystyrene micro-sphere-sized spherical colloids closely related to the experimental conditions. A numerically tractable model that quantitatively describes the separation dependence and temperature-dependent strength of DNA-mediated interactions can be used, without empirical corrections [177]. This model has been also used to successfully describe the case of grafted DNA brushes with self-interactions that compete with the inter-particle formation. This simulation design approach can propose experimentally realizable nano-structures [177], despite some criticism of this approach stating that the agreement with experiment may be fortuitous [178].

Similarly, based on standard thermodynamic arguments, a simple quantitative model for the reversible association of DNA-coated micron-sized colloids has been built [179]. These results were able to reproduce very well the experimental data regarding the dependence on temperature and sticky end coverage indicating clearly the short range of association-dissociation transition of DNA-coated colloids [176, 179, 180]. It has been shown that this transition can be described by a simple model for different

types of DNA and different DNA coverage [179]. This model takes into account the feature of the grafted DNA underlining the significance of the entropy cost due to DNA confinement onto the surface of the NPs. Here, an extensive description of the experiments carried out to validate this simple theoretical model is provided [179]. Then, a step-by-step statistical mechanics based model is developed, which is proven to describe with excellent agreement the temperature and width of the transition, which are both essential in the self-assembly of DNA-functionalized colloids [176].

A simple model for the melting and optical properties of DNA Au-NPs aggregates has been also discussed [181]. At the melting temperature, the optical properties of the aggregates change considerably, a transition that is narrower for larger NPs, as it has been also discussed elsewhere [143]. The extinction coefficient has been computed using the discrete dipole approximation, and an increasing number of bonds breaks as the temperature increases. Moreover, the melting temperature approximately corresponds to the bond percolation threshold [182]. NPs with radius of 50 nm have been considered, which compare well with experimentally used NPs. In this MC scheme, there is a reaction-limited cluster-cluster aggregation followed by dehybridization of the DNA links. These links form with a probability that depends on the temperature and the particle radius. The final structure is also a function of the number of NPs and the relaxation time. At low temperatures, one obtains clusters which after a long relaxation time transform into a compact non-fractal cluster. The optical properties [183, 184] of these structures can be estimated by using the discrete dipole approximation. Despite this structural transformation, the melting transition becomes apparent at the extinction coefficient at 520 nm wavelength remaining sharp, while the melting temperature increases with increasing NP radius as found in the previous model [181]. However, the restructuring of NPs increases the link fraction at melting to a value well above the percolation threshold. The extinction crossover compares well with experiments on Au/DNA nano-composites, where the incomplete relaxation is a robust effect. These results share similarities and may relate to a possible sol-gel transition in such aggregates [181]. Also, photo-switchable DNA-functionalized Au NPs, where hybridization is affected by the “photon dose”, can be used for tuning the DNA-mediated interactions [185], as well as high-energy Al/CuO nano-composites [186]. The optical and topological characterization of Au NP dimers linked by a single DNA double strand has been also discussed [187]. Furthermore, connected magnetic micro-particles with DNA G-quadruplexes have been recently reported in the literature [188].

A general theory for predicting the interaction potentials between DNA-coated colloids has been recently presented [189, 190]. This theory incorporates the configurational and combinatorial entropic factors that play a key role in valence-limited interactions. By enforcing self-consistency, the modelling can achieve quantitative agreement to detailed MC calculations. With suitable approximations and in particular geometries, this theory reduces to the previous successful treatments, which are now united in a common and extensible framework [189].

A theory based on an attraction of unlike particles combined with a type-independent soft-core repulsion has been realized for a binary system of DNA-functionalized colloids [191]. In an experimental system, the repulsion and attraction may be induced by a DNA solution. Based on a theoretical treatment[191], the system exhibits diverse and unusual morphologies, such as the diamond lattice and the membrane phase with an in-line square order. This is the first time, albeit theoretically, that the diamond structure has been predicted [191]. Moreover, the inverse approach has been discussed, when a particular scheme is proposed for building an arbitrary desired nano-structure. The conditions for robust self-assembly of the target structures have been identified, which includes the minimum number of “colors” needed to encode the inter-particle bonds through the hybridization of DNA pairs. Furthermore, it was shown that a floppy network with thermal fluctuations can possess an entropic rigidity and can be described as a traditional elastic solid. The onset of the entropic rigidity determines the minimal number of bond types per NP needed to encode the desired structure. This theoretical model takes into account thermodynamic considerations providing additional conditions for the occurrence of the equilibrium structures [192].

Halverson and Tkachenko [193] have studied the formation of complex mesoscopic structures with programmable local morphology and complex overall shape NPs linked with DNA. The hybridization of bonds is realized through a harmonic potential and a Poissonian statistical distribution. These results compare well with experimental results referring to the melting curve of dimers of DNA-functionalized NPs, and ordered structures in the range 5–50 nm were obtained. The key elements of this design strategy are the symmetry based on the neighbors being of different type and different sequences of bonds, the

controlled nucleation, and the cooperative binding. Based on this strategy, a number of complete nano-structures can be assembled, such as the empire state building [193]. The size limits of self-assembled colloid structures made using specific short-range interactions have been also recently discussed [194]. It has been found that structures with highly variable shapes made out of dozens of particles can form with high yield, as long as each particle in the structure binds only to the particles in their local environment [194]. Such an approach allows complete enumeration of the energy landscape and gives bounds on how large a colloidal structure can assemble with high yield. For large structures, the yield can be significant, even with hundreds of particles [194].

A theoretical discussion of a self-assembly scheme which enables the use of DNA to uniquely encode the composition and structure of micro- and nano-particle clusters has been presented in a series of papers by Licata and Tkachenko [195–198]. Several important aspects of possible experimental implementation of the proposed scheme have been discussed. For example, the competition between different types of clusters in a solution, possible jamming in an unwanted configuration, and the degeneracy due to symmetry with respect to particle permutations [195]. This methodology has been enabled from the high selectivity of DNA-mediated interactions between NPs. Based on a simple model and a more realistic description of the DNA-colloidal system, it is possible to suppress disordered glassy phases of the systems in order to obtain self-assembly into perfect crystal structures. This requires a combination of stretchable inter-particle linkers, which in a realistic situation may simply correspond to sufficiently long DNA strands, and, also, a soft repulsive potential. This approach has been implemented on a large number of cluster types and is experimentally realizable [196]. The self-assembly for the case of DNA-caged NPs has been also considered in this work [198]. The dynamics of models that contain such key-lock binding interactions, like the Watson-Crick interactions in the DNA including systems where antibodies or cell membrane proteins are grafted on NPs can be described theoretically [197]. Depending on the grafting density of the binding groups, two regimes have been predicted. In the localized regime, at low coverage, the system exhibits an exponential distribution of particle-departure times. At higher coverage, there is an interplay between departure dynamics and particle diffusion. This interplay leads to the phenomena similar to aging in glassy systems, corresponding to a sharp increase of the departure times. The diffusive effect is similar to dispersive transport in disordered semiconductors. Depending on the interaction parameters, the diffusion behavior ranges from standard to anomalous, sub-diffusive behavior [197].

Hydrodynamics may play an important role in the transformation of colloid super-lattice crystallites, especially when NPs are micron-sized [199]. For example, the spontaneous transformation through annealing from a bcc to a fcc has been experimentally observed [64, 65]. By using computer simulations and vibrational mode analysis, one can discern between different structures that have the same energy, but hydrodynamic correlations differ. It is the effect of hydrodynamics that induces anisotropic diffusion resulting in the formation of different “child” structures during the annealing processes. Therefore, structures based on DNA-functionalized NPs are not purely determined by thermodynamics, but also require the consideration of the process and properties which may be the result of hydrodynamic effects [199]. These phenomena play an important role given the narrow temperature window of the melting curve.

DNA-functionalized NPs with mobile linkers have been recently studied [56], inspired by experimental evidence [55]. This approach combines in a sense the valency of the otherwise isotropic colloids, due to the mobility of DNA linkers. By combining theoretical and simulation methods, this valency of colloids can be tuned by the nonspecific repulsion between particles. The simulations show that the resulting effective interactions lead to low-valency colloids in peculiar “open” structures, considerably different from those observed in the case of NPs with immobile DNA linkers [56].

### 3.3. Lattice models

The mapping of microscopic DNA relevant sequences onto the macroscopic phase behavior has been in the focus of theoretical and simulation work [200–202]. Such an approach should enhance the efficiency of methods detecting mutations in specific DNA sequences [200]. By using a mean-field model, the surface and bulk dissolution properties of DNA-functionalized NPs assemblies can be analyzed [201, 203]. A model for multi-component systems able to form low-symmetry ordered phases has been also proposed despite the spherical symmetry of the interactions [202]. By combining MC simulations with mean-field theory, the thermodynamic, structural and kinetic aspects of stripe phases for simple and multi-

component lattice model can be studied [202]. This lattice model represents a mixture of spherically symmetric DNA-functionalized spherical NPs with several species of DNA linkers. However, non-spherically ordered structures based on spherical NPs can also be constructed, where DNA linkers of different lengths can be used to introduce bonds of different spacing between NPs. The particular example of a stripe structure has been considered [202]. In all cases though, the system was forced to have exactly the same ground state and the highest degree of connectivity of particles. Hence, as in experiment [23], the most stable structure is the one that maximizes the number of hybridization events. However, when the strength of competitive binding is weak, a four-component system can exhibit two consecutive ordering transitions, which are due to the re-ordering of superstructures within the system. Based on those observations, an optimal design strategy has been proposed for super-structures in multi-component systems [202].

Phase transitions in DNA-linked assemblies can be described by a decorated-lattice model [204]. In this study, two types of DNA-linked colloidal mixtures have been considered, namely, systems with identical NPs functionalized with two different DNA strands and mixtures of two types of particles with each one being functionalized with different DNA strands. Establishing the similarity with Ising models with temperature and activity dependent effective interactions, various properties for these mixtures can be derived, such as the evolution of the dissolution profiles as a function of temperature and number of grafted DNA strands, in agreement with experimental systems. The increase of the dissolution temperature with the grafting density is valid only below a certain threshold. For high grafting densities, the dissolution temperature becomes a decreasing function of the DNA coverage. In systems with two different types of particles, the phase separation involves meta-stable disordered aggregates when compared to a phase transition of solvent-rich and ordered phase. The ordering of the colloidal network enhances the stability of the DNA-linked assembly resulting in the dissolution of the aggregates at higher temperatures. These results explain the contrasting evolution of the dissolution temperatures with increasing probe size in both types of mixtures [204].

A 2D lattice model for particles of many different types with short-range isotropic interactions which are pairwise specific has been also introduced [205]. The main question addressed is whether the ground state corresponding to a crystal structure is unique. Interestingly, it has been shown that it is sufficient to uniquely determine the ground state for a large class of crystal structures via MC simulations [205].

### 3.4. Genetic algorithms

An interesting approach based on genetic algorithms has been recently implemented to design DNA-grafted NPs that self-assemble into desired crystalline structures [206]. Often, the self-assembly first completes, and then the obtained self-assembly crystal structures are determined. By using genetic algorithms based on an experimentally validated evolutionary optimization methodology, it is possible to predict, not only original phase diagrams detailing the regions of known crystals, but also several new structures (for successful applications of evolutionary algorithms in soft matter systems with directional bonding see [207–210]). The agreement of these results with the existing experimentally predicted structures validates the use of this tool for the design of materials based on this genetic technique [206]. Although the traditional approach is very useful in order to validate the results, genetic algorithms offer a way of designing crystal structures with desired properties, determining in this way the desired structure that underlies those properties. In an example where two types of colloids are grafted with complementary ssDNA sequences, ordered colloidal crystals have been obtained. This methodology is generalizable, fast, and selective, able at the same time to reproduce parameters relevant to four currently realized crystals and unobserved structures [206].

### 3.5. Atomistic simulations

Atomistic simulations of 2 nm Au truncated octahedral NPs functionalized with four single-stranded DNA chains have been also realized [52, 211]. However, such an approach is limited to a small number of short DNA chains similarly to the model of Starr and Sciortino [142], which deviates considerably from an experimentally realized nano-structure. However, in this study the authors have explored the possibility of hydrogen bonds between the adsorbed ssDNAs, finding that there is not a significant amount

of hydrogen bonds. This conclusion is consistent with the observed increase of the melting temperature [52, 211].

Despite the extensive use of coarse-grained models, a million-atom MD simulation has been used to study the formation of bcc and fcc super-crystals of DNA-functionalized Au NPs [212]. The bcc crystal contained 2.77 million atoms, whereas the fcc contained 5.05, with the diameter of the NP being 3 nm. After 10 ns DNA structures vary smoothly, while the ion distributions around DNAs can also be estimated. Analysis of these results shows that ions bind stronger in bcc structures than in fcc structures. This effect explains the higher melting temperature of bcc structures and underlines the significance of entropic effects in fcc structures. In this work, the Young's and bulk moduli of the obtained super-crystals have been also obtained. Note that the Poisson ratios for both super-crystals were close to the ideal value, that is 1/3 [212].

### 3.6. Simulations of anisotropic nanoparticles

Anisotropic NPs grafted with DNA have recently appeared in the literature for the case of nano-cubes [213], where the phase diagram similarly to the previous work with coated spherical NPs has been studied [83, 158]. These nano-cubes are capable of self-assembling into crystalline, liquid crystalline, rotator, or non-crystalline phases with both long-range positional and orientational order [213].

## 4. Combined simulation and experimental studies

The growth dynamics for DNA-mediated NP crystallization has been one of the fundamental questions, because during the formation of crystalline-structure NPs become kinetically trapped. Moreover, it has been found that the growth of isolated crystallites is described by the power law  $\sim t^{1/2}$  [214]. The coalescence of these crystallites significantly slows down the growth process due to the orientational mismatch of the crystallites. MD simulations show that the misorientation angle decreases continuously during the coalescence, which is a signature of a rotation induced coalescence mechanism. The coarsening of the conformation at the boundary between coalescing crystallites takes place after the orientation of the crystals. When nucleotide chains are larger, the dynamics become faster due to the enhanced surface diffusion, which more effectively reduces the curvature at the boundary of two super-lattices. These results have provided fundamental understanding on the relationship between NP surface chemistry and its crystallite growth and coalescence [214].

A quantitative prediction of the associated thermodynamics and kinetics of DNA-coated particles considering different functionalization schemes has been discussed by Leunissen et al. [215]. Preparation, structural, and optical features of 2D cross-linked DNA/Au NP conjugates have been also considered in the literature [216, 217], as well as the tuning of ratios, densities and supra-molecular spacing in bi-functional DNA-modified Au NPs [218]. Experimental results [215] show that the suspension behavior is very sensitive to the grafting details, such as the length and flexibility of the DNA strands, as well as the surface coverage. Therefore, in order to control the assembly process, emphasis should be put on the structural and dynamical features of the DNA coatings. By varying the temperature cycle, beads concentration, and surface coverage, the association-dissociation dynamics and kinetics can be studied systematically. Moreover, the tethered backbone segments onto the NPs' surface has been found to play an important role in the association-dissociation properties, since they affect the total number of inter-particle bonds and, as a result, the configurational entropy cost associated with these bonds. Independently of the tether backbone, self-complementary palindromic sticky ends can easily form intra-particle hairpins and loops considerably altering the association behavior. Hairpin DNA-functionalized Au colloids have found also application in the imaging of mRNA in living cells [219]. Such structures are more important during faster temperature quenches, lower concentration and lower surface coverage. Other applications include the design of "self-protected" DNA-mediated interactions, which enable more versatile self-assembly schemes [215].

Self-replicating materials of DNA-functionalized colloids are also interesting [220]. Such systems exploit the strong specificity and thermal reversibility for the interactions between DNA-functionalized NPs. The fundamental behavior of the self-replicating process related to the equilibrium and kinetic aspects

of aggregation-dissociation behavior of particles has been determined via experimental methods. It has also been found that the dissociation temperature is very sharp, occurring unexpectedly at low temperatures. When the fraction of the sticky ends becomes smaller, the dissociation temperature shifts to even lower scales. The sharpness of the transition and the fraction of sticky ends are important parameters in this self-replication scheme. Moreover, a double-stranded backbone prevents unwanted hybridization events, such as secondary structure formation, which leads to peculiar aggregation kinetics. This is due to the competition between inter- and intra-hybridization events. Additionally, by functionalizing a single particle species with two distinct DNA sequences, permanent bonds can form [220].

The bending dynamics of DNA-linked colloidal particle chains have been also studied [221] by using a worm-like chain (WLC) model to represent the grafted DNA strands onto the NPs surface, analogously to the case of semi-flexible linear polymers. The persistence length of these grafted DNA chains can be determined by monitoring the thermal fluctuations of the chains. In this way, these lengths can be tuned within a large range from 1 to 50 nm, which corresponds to a linking length of DNA of 75 to 15 bases. Interestingly, the bending relaxation dynamics of these chains matches the theoretical predictions, suggesting the use of such a WLC DNA model approach for both equilibrium and dynamical studies [221].

Park et al. [222] investigated the structure of NPs aggregates at room temperature by combining theoretical and experimental methods. Experimental methods involve extinction spectroscopy measurements and dynamic light scattering, where Au NPs have sizes between 60 and 80 nm and DNA strands of about 30 base-pairs. Theoretical studies use calculated spectra for models of the aggregate structures to determine the structure that matches the observations. Since particles in this study are larger than particles used previously, there is a higher sensitivity of spectra to aggregate structures. Combining theoretical and experimental results in the range where the highest agreement was found, it was argued that DNA hybridization takes place under irreversible conditions at room temperature. The model also takes into account other effects, such as the poly-dispersity in the size of NPs and lattice defects. The room temperature aggregate is always a fractal, and a morphological change from fractal towards compact structures occurs below the melting temperature [222].

The kinetics of DNA-coated sticky particles through the exploration of a number of properties have been studied by Wu et al. [223]. The aggregation rate, which depends on the rate of NPs encounter and the probability that such an encounter results in the sticking of the particle, has been studied. Contrary to the previous toy models [23], this one takes into account a possibility of hybridization. By combining experimental and theoretical techniques, the aggregation times of micron-sized particles as a function of DNA coverage and salt concentration have been obtained. A simple model using reaction-limited kinetics and experimental oligomer hybridization rates is in very good agreement with the experimental data. The Coulomb barrier at the nanometer scale retarding DNA hybridization is a significant controlling factor of the association process. This model also allows an easy measurement of microscopic hybridization rates from macroscopic aggregation, thus enabling the design of complex self-assembly schemes with a controlled kinetics [223].

## 5. Synopsis

To summarize, there has been a great advancement in understanding the self-assembly of DNA-functionalized NPs. A large number of crystalline structures can be fabricated and the effects of various parameters influencing the self-assembly are now well-understood. During the last years, a wealth of different uses of DNA-functionalized NPs has been realized on the basis of different applications. However, the control of self-assembly and crystallization kinetics remains still an unresolved issue. This problem leads to kinetically trapped structures, one of the main reasons behind the difficulty in fabricating long-range stable crystalline structures and the efficient growth of crystalline structures on substrates [17]. Problems in synthesis of these NPs in a controllable and predictable way is also a concern [17]. Additionally, transitioning DNA-engineered NP super-lattices from solution to the solid state is challenging [224]. Steps toward creating dynamic self-assembly materials, that is materials which are capable of changing their crystalline structure in a controlled way due to specific stimuli, have been also taken [17, 225]. Recently, dynamically interchangeable NP super-lattices have been produced via the use of nucleic acid allosteric effectors [226]. This approach has been suggested for fcc, bcc, CsCl and AlB<sub>2</sub> crystal symmetries

[226]. Another open question is the design of DNA-functionalized NPs that could lead to the formation of single-component non-compact diamond structures. Although some theoretical suggestions exist along these lines, this structure has not been realized experimentally, or by any simulation work. Moreover, given the large flexibility of DNA, the formation of single-component diamond structures with small NPs may not be possible [156]. An opportunity window could be opened via the design with NPs of non-spherical shape which has been the topic of recent experimental [109, 110] and simulation work [213].

## Acknowledgements

PET, GK and CD acknowledge financial support by the Austrian Research Foundation (FWF) under Proj. No. F41 (SFB ViCoM). In addition, GK acknowledges financial support by the FWF under Proj. No. P23910–N16.

## References

1. Crocker J.C., *Nature*, 2008, **451**, 528; doi:10.1038/451528a.
2. Travesset A., *Science*, 2011, **334**, No. 6053, 183; doi:10.1126/science.1213070.
3. Rogers W.B., Manoharan V.N., *Science*, 2015, **347**, 639; doi:10.1126/science.1259762.
4. Hurst S.J., Hill H.D., Macfarlane R.J., Wu J., Dravid V.P., Mirkin C.A., Small, 2009, **5**, No. 19, 2156; doi:10.1002/smll.200900568.
5. Biomedical Nanotechnology: Methods and Protocols, Hurst S.J. (Ed.), Springer Protocols, Methods in Molecular Biology Series, Humana Press, New York, 2011.
6. DNA Nanotechnology: Methods and Protocols, Zuccheri G., Samori B. (Eds.), Springer Protocols, Methods in Molecular Biology Series, Humana Press, New York, 2011.
7. Heuer-Jungemann A., Harimech P.K., Brown T., Kanaras A.G., *Nanoscale*, 2013, **5**, No. 20, 9503; doi:10.1039/c3nr03707j.
8. Rosi N.L., Mirkin C.A., *Chem. Rev.*, 2005, **105**, No. 4, 1547; doi:10.1021/cr030067f.
9. Sokolova V., Epple M., *Angew. Chem. Int. Edit.*, 2008, **47**, No. 8, 1382; doi:10.1002/anie.200703039.
10. Tan S.J., Campolongo M.J., Luo D., Cheng W., *Nat. Nanotechnol.*, 2011, **6**, 268; doi:10.1038/nnano.2011.49.
11. Rosi N.L., Giljohann D.A., Thaxton C.S., Lytton-Jean A.K., Han M.S., Mirkin C.A., *Science*, 2006, **312**, No. 5776, 1027; doi:10.1126/science.1125559.
12. Niemeyer C.M., *Angew. Chem. Int. Edit.*, 2001, **40**, 4128; doi:10.1002/1521-3773(20011119)40:22<4128::AID-ANIE4128>3.0.CO;2-S.
13. Macfarlane R.J., Thaner R.V., Brown K.A., Zhang J., Lee B., Nguyen S.T., Mirkin C.A., *Proc. Natl. Acad. Sci. USA*, 2014, **111**, No. 42, 14995; doi:10.1073/pnas.1416489111.
14. Alivisatos A.P., Johnsson K.P., Peng X., Wilson T.E., Loweth C.J., Bruchez (Jr.) M.P., Schultz P.G., *Nature*, 1996, **382**, 609; doi:10.1038/382609a0.
15. Mirkin C.A., Letsinger R.L., Mucic R.C., Storhoff J.J., *Nature*, 1996, **382**, 607; doi:10.1038/382607a0.
16. Hurst S.J., Hill H.D., Mirkin C.A., *J. Am. Chem. Soc.*, 2008, **130**, No. 36, 12192; doi:10.1021/ja804266j.
17. Macfarlane R.J., O'Brien M.N., Petrosko S.H., A. M.C., *Angew. Chem. Int. Edit.*, 2013, **52**, 5688; doi:10.1002/anie.201209336.
18. Norris D.J., *Nat. Mater.*, 2007, **6**, 177; doi:10.1038/nmat1844.
19. Barrow S.J., Funston A.M., Wei X., Mulvaney P., *Nano Today*, 2013, **8**, No. 2, 138; doi:10.1016/j.nantod.2013.02.005.
20. Geerts N., Eiser E., *Soft Matter*, 2010, **6**, No. 19, 4647; doi:10.1039/c001603a.
21. Hung A.M., Noh H., Cha J.N., *Nanoscale*, 2010, **2**, No. 12, 2530; doi:10.1039/c0nr00430h.
22. Katz E., Willner I., *Angew. Chem. Int. Edit.*, 2004, **43**, No. 45, 6042; doi:10.1002/anie.200400651.
23. Macfarlane R.J., Lee B., Jones M.R., Harris N., Schatz G.C., Mirkin C.A., *Science*, 2011, **334**, No. 6053, 204; doi:10.1126/science.1210493.
24. Mazid R.R., Si K.J., Cheng W., *Methods*, 2014, **67**, No. 2, 215; doi:10.1016/j.ymeth.2014.01.017.
25. Storhoff J.J., Mirkin C.A., *Chem. Rev.*, 1999, **99**, No. 7, 1849; doi:10.1021/cr970071p.
26. Pérez A., Luque F.J., Orozco M., *Acc. Chem. Res.*, 2011, **45**, No. 2, 196; doi:10.1021/ar2001217.
27. Li N.K., Kim H.S., Nash J.A., Lim M., Yingling Y.G., *Mol. Simulat.*, 2014, **40**, 777; doi:10.1080/08927022.2014.913792.
28. Di Michele L., Eiser E., *Phys. Chem. Chem. Phys.*, 2013, **15**, No. 9, 3115; doi:10.1039/c3cp43841d.
29. Zhang X., Wang R., Xue G., *Soft Matter*, 2015, doi:10.1039/C4SM02649G.

30. Cao Y., Jin R., Mirkin C.A., *J. Am. Chem. Soc.*, 2001, **123**, No. 32, 7961; doi:10.1021/ja011342n.
31. Macfarlane R.J., Jones M.R., Senesi A.J., Young K.L., Lee B., Wu J., Mirkin C.A., *Angew. Chem. Int. Edit.*, 2010, **49**, No. 27, 4589; doi:10.1002/anie.201000633.
32. Ueberschär O., Wagner C., Stangner T., Gutsche C., Kremer F., *Polymer*, 2011, **52**, No. 8, 1829; doi:10.1016/j.polymer.2011.02.001.
33. Jones M.R., Osberg K.D., Macfarlane R.J., Langille M.R., Mirkin C.A., *Chem. Rev.*, 2011, **111**, 3736; doi:10.1021/cr1004452.
34. Fan J.A., He Y., Bao K., Wu C., Bao J., Schade N.B., Manoharan V.N., Shvets G., Nordlander P., Liu D.R., Capasso F., *Nano Lett.*, 2011, **11**, No. 11, 4859; doi:10.1021/nl203194m.
35. Baker B.A., Milam V.T., *Langmuir*, 2010, **26**, No. 12, 9818; doi:10.1021/la100077f.
36. Sebba D.S., Mock J.J., Smith D.R., LaBean T.H., Lazarides A.A., *Nano Lett.*, 2008, **8**, No. 7, 1803; doi:10.1021/nl080029h.
37. Soto C.M., Srinivasan A., Ratna B.R., *J. Am. Chem. Soc.*, 2002, **124**, No. 29, 8508; doi:10.1021/ja017653f.
38. Feng L., Dreyfus R., Sha R., Seeman N.C., Chaikin P.M., *Adv. Mater.*, 2013, **25**, No. 20, 2779; doi:10.1002/adma.201204864.
39. Johnston A.P., Caruso F., *Angew. Chem. Int. Edit.*, 2007, **46**, No. 15, 2677; doi:10.1002/anie.200605135.
40. Hussain N., *Int. J. Pharm.*, 2003, **254**, No. 1, 27; doi:10.1016/S0378-5173(02)00672-5.
41. Jiang X., Qu W., Pan D., Ren Y., Williford J.M., Cui H., Luijten E., Mao H.Q., *Adv. Mater.*, 2013, **25**, No. 2, 227; doi:10.1002/adma.201202932.
42. Singh A., Eksiri H., Yingling Y.G., *J. Polym. Sci. Pt. B-Polym. Phys.*, 2011, **49**, No. 22, 1563; doi:10.1002/polb.22349.
43. Geerts N., Schmatko T., Eiser E., *Langmuir*, 2008, **24**, No. 9, 5118; doi:10.1021/la7036789.
44. Dave N., Liu J., *Adv. Mater.*, 2011, **23**, No. 28, 3182; doi:10.1002/adma.201101086.
45. Dave N., Liu J., *ACS Nano*, 2011, **5**, No. 2, 1304; doi:10.1021/nn1030093.
46. Peled D., Naaman R., Daube S.S., *J. Phys. Chem. B*, 2010, **114**, No. 25, 8581; doi:10.1021/jp104533q.
47. Heuer-Jungemann A., Kirkwood R., El-Sagheer A.H., Brown T., Kanaras A.G., *Nanoscale*, 2013, **5**, No. 16, 7209; doi:10.1039/c3nr02362a.
48. Chen T., Wu C.S., Jimenez E., Zhu Z., Dajac J.G., You M., Han D., Zhang X., Tan W., *Angew. Chem. Int. Edit.*, 2013, **52**, 2012; doi:10.1002/anie.201209440.
49. Zhang K., Hao L., Hurst S.J., Mirkin C.A., *J. Am. Chem. Soc.*, 2012, **134**, No. 40, 16488; doi:10.1021/ja306854d.
50. Seferos D.S., Giljohann D.A., Hill H.D., Prigodich A.E., Mirkin C.A., *J. Am. Chem. Soc.*, 2007, **129**, No. 50, 15477; doi:10.1021/ja0776529.
51. Xin A., Dong Q., Xiong C., Ling L., *Chem. Commun.*, 2009, No. 13, 1658; doi:10.1039/b815825h.
52. Lee O.S., Prytkova T.R., Schatz G.C., *J. Phys. Chem. Lett.*, 2010, **1**, No. 12, 1781; doi:10.1021/jz100435a.
53. Zhang C., Macfarlane R.J., Young K.L., Choi C.H.J., Hao L., Auyeung E., Liu G., Zhou X., Mirkin C.A., *Nat. Mater.*, 2013, **12**, 741; doi:10.1038/nmat3647.
54. Zhang Y., Lu F., Yager K.G., van der Lelie D., Gang O., *Nat. Nanotechnol.*, 2013, **8**, 865; doi:10.1038/nnano.2013.209.
55. Van der Meulen S.A., Leunissen M.E., *J. Am. Chem. Soc.*, 2013, **135**, No. 40, 15129; doi:10.1021/ja406226b.
56. Angioletti-Uberti S., Varilly P., Mognetti B.M., Frenkel D., *Phys. Rev. Lett.*, 2014, **113**, 128303; doi:10.1103/PhysRevLett.113.128303.
57. Lee J.S.H., Lytton-Jean A.K., Hurst S.J., Mirkin C.A., *Nano Lett.*, 2007, **7**, No. 7, 2112; doi:10.1021/nl071108g.
58. Han J., Ohara S., Sato K., Xu H., Tan Z., Morisada Y., Kuruma K., Naito M., Shan P., Umetsu M., *Mater. Lett.*, 2012, **79**, 78; doi:10.1016/j.matlet.2012.03.094.
59. Lee J.S.H., Stoeva S.I., Mirkin C.A., *J. Am. Chem. Soc.*, 2006, **128**, No. 27, 8899; doi:10.1021/ja061651j.
60. Yang J., Lee J.Y., Too H.P., Chow G.M., Gan L.M., *Chem. Phys.*, 2006, **323**, No. 2-3, 304; doi:10.1016/j.chemphys.2005.09.044.
61. Chen Y., Mao C., *Small*, 2008, **4**, No. 12, 2191; doi:10.1002/smll.200800569.
62. Kim G.A., Han S.H., Lee J.S., *Mater. Lett.*, 2012, **68**, 118; doi:10.1016/j.matlet.2011.10.058.
63. Kim J.Y., Lee J.S.H., *Nano Lett.*, 2009, **9**, No. 12, 4564; doi:10.1021/nl9030709.
64. Casey M.T., Scarlett R.T., Rogers W.B., Jenkins I., Sinno T., Crocker J.C., *Nat. Commun.*, 2012, **3**, 1209; doi:10.1038/ncomms2206.
65. Nykypanchuk D., Maye M.M., van der Lelie D., Gang O., *Nature*, 2008, **451**, No. 7178, 549; doi:10.1038/nature06560.
66. Dillenback L.M., Goodrich G.P., Keating C.D., *Nano Lett.*, 2006, **6**, No. 1, 16; doi:10.1021/nl0508873.
67. Srivastava S., Nykypanchuk D., Maye M.M., Tkachenko A.V., Gang O., *Soft Matter*, 2013, **9**, No. 44, 10452; doi:10.1039/c3sm51289d.
68. Maye M.M., Kumara M.T., Nykypanchuk D., Sherman W.B., Gang O., *Nat. Nanotechnol.*, 2010, **5**, 116; doi:10.1038/nnano.2009.378.

69. Macfarlane R.J., Lee B., Hill H.D., Senesi A.J., Seifert S., Mirkin C.A., Proc. Natl. Acad. Sci. USA, 2009, **106**, No. 26, 10493; doi:10.1073/pnas.0900630106.
70. Senesi A.J., Eichelsdoerfer D.J., Macfarlane R.J., Jones M.R., Auyeung E., Lee B., Mirkin C.A., Angew. Chem. Int. Edit., 2013, **52**, No. 26, 6624; doi:10.1002/anie.201301936.
71. Auyeung E., Cutler J.I., Macfarlane R.J., Jones M.R., Wu J., Liu G., Zhang K., Osberg K.D., Mirkin C.A., Nat. Nanotechnol., 2012, **7**, 24; doi:10.1038/nnano.2011.222.
72. Keegan G.L., Aherne D., Defrancq E., Gun'ko Y.K., Kelly J.M., J. Phys. Chem. C, 2013, **117**, No. 1, 669; doi:10.1021/jp309449d.
73. Valignat M.P., Theodoly O., Crocker J.C., Russel W.B., Chaikin P.M., Proc. Natl. Acad. Sci. USA, 2005, **102**, No. 12, 4225; doi:10.1073/pnas.0500507102.
74. Shin J., Zhang X., Liu J., J. Phys. Chem. B, 2012, **116**, No. 45, 13396; doi:10.1021/jp310662m.
75. Hill H.D., Macfarlane R.J., Senesi A.J., Lee B., Park S.J., Mirkin C.A., Nano Lett., 2008, **8**, No. 8, 2341; doi:10.1021/nl8011787.
76. Storhoff J.J., Elghanian R., Mirkin C.A., Letsinger R.L., Langmuir, 2002, **18**, No. 17, 6666; doi:10.1021/la0202428.
77. Doyen M., Bartik K., Bruylants G., Polymers, 2013, **5**, No. 3, 1041; doi:10.3390/polym5031041.
78. Park S.Y., Lytton-Jean A.K., Lee B., Weigand S., Schatz G.C., Mirkin C.A., Nature, 2008, **451**, No. 7178, 553; doi:10.1038/nature06508.
79. Milam V.T., Hiddessen A.L., Crocker J.C., Graves D.J., Hammer D.A., Langmuir, 2003, **19**, No. 24, 10317; doi:10.1021/la034376c.
80. Lubitz I., Kotlyar A., Bioconjugate Chem., 2011, **22**, No. 10, 2043; doi:10.1021/bc200257e.
81. Xiong H., van der Lelie D., Gang O., J. Am. Chem. Soc., 2008, **130**, No. 8, 2442; doi:10.1021/ja710710j.
82. Xiong H., van der Lelie D., Gang O., Phys. Rev. Lett., 2009, **102**, 015504; doi:10.1103/PhysRevLett.102.015504.
83. Knorowski C., Burleigh S., Travesset A., Phys. Rev. Lett., 2011, **106**, No. 21, 215501; doi:10.1103/PhysRevLett.106.215501.
84. Cigler P., Lytton-Jean A.K., Anderson D.G., Finn M.G., Park S.J., Nat. Mater., 2010, **9**, 918; doi:10.1038/nmat2877.
85. Park S.J., Lazarides A.A., Mirkin C.A., Letsinger R.L., Angew. Chem. Int. Edit., 2001, **40**, No. 15, 2909; doi:10.1002/1521-3773(20010803)40:15<2909::AID-ANIE2909>3.0.CO;2-O.
86. Park S.J., Lazarides A.A., Storhoff J.J., Pesce L., Mirkin C.A., J. Phys. Chem. B, 2004, **108**, No. 33, 12375; doi:10.1021/jp040242b.
87. Qin W.J., Yung L.Y.L., Langmuir, 2005, **21**, No. 24, 11330; doi:10.1021/la051630n.
88. Strable E., Johnson J.E., Finn M.G., Nano Lett., 2004, **4**, No. 8, 1385; doi:10.1021/nl0493850.
89. Sun D., Gang O., J. Am. Chem. Soc., 2011, **133**, No. 14, 5252; doi:10.1021/ja111542t.
90. McGinley J.T., Jenkins I., Sinno T., Crocker J.C., Soft Matter, 2013, **9**, No. 38, 9119; doi:10.1039/c3sm50950h.
91. Nykypanchuk D., Maye M.M., van der Lelie D., Gang O., Langmuir, 2007, **23**, No. 11, 6305; doi:10.1021/la0637566.
92. Kim A.J., Biancaniello P.L., Crocker J.C., Langmuir, 2006, **22**, No. 5, 1991; doi:10.1021/la0528955.
93. Kim A.J., Scarlett R.T., Biancaniello P.L., Sinno T., Crocker J.C., Nat. Mater., 2009, **8**, 52; doi:10.1038/nmat2338.
94. Rogers P.H., Michel E., Bauer C.A., Vanderet S., Hansen D., Roberts B.K., Calvez A., Crews J.B., Lau K.O., Wood A., Pine D.J., Schwartz P.V., Langmuir, 2005, **21**, No. 12, 5562; doi:10.1021/la046790y.
95. Rogers W.B., Sinno T., Crocker J.C., Soft Matter, 2013, **9**, No. 28, 6412; doi:10.1039/c3sm50593f.
96. Biancaniello P., Kim A., Crocker J., Phys. Rev. Lett., 2005, **94**, No. 5, 058302; doi:10.1103/PhysRevLett.94.058302.
97. Biancaniello P.L., Crocker J.C., Hammer D.A., Milam V.T., Langmuir, 2007, **23**, No. 5, 2688; doi:10.1021/la062885j.
98. Kegler K., Salomo M., Kremer F., Phys. Rev. Lett., 2007, **98**, No. 5, 058304; doi:10.1103/PhysRevLett.98.058304.
99. Kegler K., Konieczny M., Dominguez-Espinosa G., Gutsche C., Salomo M., Kremer F., Likos C.N., Phys. Rev. Lett., 2008, **100**, No. 11, 118302; doi:10.1103/PhysRevLett.100.118302.
100. Chollakup R., Smithipong W., Chworo A., Polym. Chem., 2010, **1**, No. 5, 658; doi:10.1039/b9py00290a.
101. Scarlett R.T., Crocker J.C., Sinno T., J. Chem. Phys., 2010, **132**, No. 23, 234705; doi:10.1063/1.3453704.
102. Scarlett R.T., Ung M.T., Crocker J.C., Sinno T., Soft Matter, 2011, **7**, No. 5, 1912; doi:10.1039/c0sm00370k.
103. Leunissen M.E., Dreyfus R., Cheong F.C., Grier D.G., Sha R., Seeman N.C., Chaikin P.M., Nat. Mater., 2009, **8**, No. 7, 590; doi:10.1038/nmat2471.
104. Feng L., Sha R., Seeman N.C., Chaikin P.M., Phys. Rev. Lett., 2012, **109**, No. 18, 188301; doi:10.1103/PhysRevLett.109.188301.
105. Claridge S.A., Goh S.L., Frechet J.M.J., Williams S.C., Micheel C.M., Alivisatos A.P., Chem. Mater., 2005, **17**, No. 7, 1628; doi:10.1021/cm0484089.
106. Maye M.M., Nykypanchuk D., van der Lelie D., Gang O., J. Am. Chem. Soc., 2006, **128**, No. 43, 14020; doi:10.1021/ja0654229.
107. Maye M.M., Nykypanchuk D., van der Lelie D., Gang O., Small, 2007, **3**, No. 10, 1678; doi:10.1002/smll.200700357.
108. Cutler J.I., Zhang K., Zheng D., Auyeung E., Prigodich A.E., Mirkin C.A., J. Am. Chem. Soc., 2011, **133**, No. 24, 9254; doi:10.1021/ja203375n.

109. Jones M.R., Macfarlane R.J., Prigodich A.E., Patel P.C., Mirkin C.A., *J. Am. Chem. Soc.*, 2011, **133**, No. 46, 18865; doi:10.1021/ja206777k.
110. Jones M.R., Macfarlane R.J., Lee B., Zhang J., Young K.L., Senesi A.J., Mirkin C.A., *Nat. Mater.*, 2010, **9**, 913; doi:10.1038/nmat2870.
111. Dujardin E., Hsin L.B., Wang C., Mann S., *Chem. Commun.*, 2001, No. 14, 1264; doi:10.1039/b102319p.
112. Geerts N., Schreck C.F., Beales P.A., Shigematsu H., O'Hern C.S., Vanderlick T.K., *Langmuir*, 2013, **29**, No. 42, 13089; doi:10.1021/la403091w.
113. Tan L.H., Xing H., Chen H., Lu Y., *J. Am. Chem. Soc.*, 2013, **135**, No. 47, 17675; doi:10.1021/ja408033e.
114. Qin W.J., Yung L.Y.L., *Bioconjugate Chem.*, 2008, **19**, 385; doi:10.1021/bc700178f.
115. Zhang J., Liu Y., Ke Y., Yan H., *Nano Lett.*, 2006, **6**, No. 2, 248; doi:10.1021/nl052210l.
116. Pinto Y.Y., Le J.D., Seeman N.C., Musier-Forsyth K., Taton T.A., Kiehl R.A., *Nano Lett.*, 2005, **5**, No. 12, 2399; doi:10.1021/nl0515495.
117. Millstone J.E., Georganopoulou D.G., Xu X.Y., Wei W., Li S.Y., Mirkin C.A., *Small*, 2008, **4**, No. 12, 2176; doi:10.1002/smll.200800931.
118. Young K.L., Jones M.R., Zhang J., Macfarlane R.J., Esquivel-Sirvent R., Nap R.J., Wu J., Schatz G.C., Lee B., Mirkin C.A., *Proc. Natl. Acad. Sci. USA*, 2012, **109**, No. 7, 2240; doi:10.1073/pnas.1119301109.
119. Maye M.M., Nykypanchuk D., Cuisinier M., van der Lelie D., Gang O., *Nat. Mater.*, 2009, **8**, 388; doi:10.1038/nmat2421.
120. Xing H., Wang Z., Xu Z., Xiang Y., Liu G.L., Lu Y., *ACS Nano*, 2012, **6**, No. 1, 802; doi:10.1021/nn2042797.
121. Xu X., Rosi N.L., Wang Y., Huo F., Mirkin C.A., *J. Am. Chem. Soc.*, 2006, **128**, No. 29, 9286; doi:10.1021/ja061980b.
122. Cederquist K.B., Keating C.D., *ACS Nano*, 2009, **3**, No. 2, 256; doi:10.1021/nn9000726.
123. Vial S., Nykypanchuk D., Yager K.G., Tkachenko A.V., Gang O., *ACS Nano*, 2013, **7**, No. 6, 5437; doi:10.1021/nn401413b.
124. Jahn S., Geerts N., Eiser E., *Langmuir*, 2010, **26**, No. 22, 16921; doi:10.1021/la103192q.
125. Cheng W., Campolongo M.J., Cha J.J., Tan S.J., Umbach C.C., Muller D.A., Luo D., *Nat. Mater.*, 2009, **8**, No. 8, 519; doi:10.1038/nmat2440.
126. Lan X., Chen Z., Liu B.J., Ren B., Henzie J., Wang Q., *Small*, 2013, **9**, No. 13, 2308; doi:10.1002/smll.201202503.
127. Geerts N., Eiser E., *Soft Matter*, 2010, **6**, No. 3, 664; doi:10.1039/B917846E.
128. Estephan Z.G., Qian Z., Lee D., Crocker J.C., Park S.J., *Nano Lett.*, 2013, **13**, No. 9, 4449; doi:10.1021/nl4023308.
129. Hung A.M., Micheel C.M., Bozano L.D., W. O.L., Wallraff G.M., Cha J.N., *Nat. Nanotechnol.*, 2010, **5**, 121; doi:10.1038/nnano.2009.450.
130. Taton T.A., Mucic R.C., Mirkin C.A., Letsinger R.L., *J. Am. Chem. Soc.*, 2000, **122**, No. 26, 6305; doi:10.1021/ja0007962.
131. Shyr M.H.S., Wernette D.P., Wiltzius P., Lu Y., Braun P.V., *J. Am. Chem. Soc.*, 2008, **130**, No. 26, 8234; doi:10.1021/ja711026r.
132. DeMille R.C., Cheatham III T.E., Molinero V., *J. Phys. Chem. B*, 2011, **115**, No. 1, 132; doi:10.1021/jp107028n.
133. Kenward M., Dorfman K.D., *J. Chem. Phys.*, 2009, **130**, No. 9, 095101; doi:10.1063/1.3078795.
134. Drukker K., Wu G., Schatz G.C., *J. Chem. Phys.*, 2001, **114**, No. 1, 579; doi:10.1063/1.1329137.
135. Knotts T.A.t., Rathore N., Schwartz D.C., de Pablo J.J., *J. Chem. Phys.*, 2007, **126**, No. 8, 084901; doi:10.1063/1.2431804.
136. Sambriski E.J., Schwartz D.C., de Pablo J.J., *Biophys. J.*, 2009, **96**, No. 5, 1675; doi:10.1016/j.bpj.2008.09.061.
137. Lequieu J.P., Hinckley D.M., de Pablo J.J., *Soft Matter*, 2015, **11**, 1919; doi:10.1039/C4SM02573C.
138. Linak M.C., Tourdot R., Dorfman K.D., *J. Chem. Phys.*, 2011, **135**, No. 20, 205102; doi:10.1063/1.3662137.
139. Mladek B.M., Fornleitner J., Martinez-Veracoechea F.J., Dawid A., Frenkel D., *Soft Matter*, 2013, **9**, No. 30, 7342; doi:10.1039/c3sm50701g.
140. Ding Y., Mittal J., *J. Chem. Phys.*, 2014, **141**, No. 18, 184901; doi:10.1063/1.4900891.
141. Sales-Pardo M., Guimerá R., Moreira A., Widom J., Amaral L., *Phys. Rev. E*, 2005, **71**, No. 5, 051902; doi:10.1103/PhysRevE.71.051902.
142. Starr F.W., Sciortino F., *J. Phys.: Condens. Matter*, 2006, **18**, No. 26, L347; doi:10.1088/0953-8984/18/26/L02.
143. Theodorakis P.E., Dellago C., Kahl G., *J. Chem. Phys.*, 2013, **138**, No. 2, 025101; doi:10.1063/1.4773920.
144. Lara V.F., Starr F.W., *Soft Matter*, 2011, **7**, No. 5, 2085; doi:10.1039/c0sm00989j.
145. Padovan-Merhar O., Lara F.V., Starr F.W., *J. Chem. Phys.*, 2011, **134**, No. 24, 244701; doi:10.1063/1.3596745.
146. Largo J., Starr F.W., Sciortino F., *Langmuir*, 2007, **23**, No. 11, 5896; doi:10.1021/la063036z.
147. Dai W., Hsu C.W., Sciortino F., Starr F.W., *Langmuir*, 2010, **26**, No. 5, 3601; doi:10.1021/la903031p.
148. Dai W., Kumar S.K., Starr F.W., *Soft Matter*, 2010, **6**, No. 24, 6130; doi:10.1039/c0sm00484g.
149. Hsu C.W., Largo J., Sciortino F., Starr F.W., *Proc. Natl. Acad. Sci. USA*, 2008, **105**, No. 37, 13711; doi:10.1073/pnas.0804854105.
150. Flory P., *Principles of Polymer Chemistry*, Cornell University Press, New York, 1953.

151. Stockmayer W.H., J. Chem. Phys., 1943, **11**, No. 45; doi:10.1063/1.1723803.
152. Hsu C.W., Sciortino F., Starr F.W., Phys. Rev. Lett., 2010, **105**, No. 5, 055502; doi:10.1103/PhysRevLett.105.055502.
153. Seifpour A., Dahl S.R., Jayaraman A., Mol. Simulat., 2014, **40**, No. 14, 1085; doi:10.1080/08927022.2013.845888.
154. Seifpour A., Dahl S.R., Lin B., Jayaraman A., Mol. Simulat., 2013, **39**, No. 9, 741; doi:10.1080/08927022.2013.765569.
155. Chi C., Lara V.F., Tkachenko A.V., Starr F.W., Gang O., ACS Nano, 2012, **6**, No. 8, 6793; doi:10.1021/nn301528h.
156. Rovigatti L., Smallenburg F., Romano F., Sciortino F., ACS Nano, 2014, **8**, No. 4, 3567; doi:10.1021/nn501138w.
157. Rovigatti L., Bomboi F., Sciortino F., J. Chem. Phys., 2014, **140**, 154903; doi:10.1063/1.4870467.
158. Knorowski C., Travesset A., Curr. Opin. Solid State Mat. Sci., 2011, **15**, No. 6, 262; doi:10.1016/j.cossms.2011.07.002.
159. Knorowski C., Travesset A., Soft Matter, 2012, **8**, No. 48, 12053; doi:10.1039/c2sm26832a.
160. Li T.I., Sknepnek R., Macfarlane R.J., Mirkin C.A., de la Cruz M.O., Nano Lett., 2012, **12**, No. 5, 2509; doi:10.1021/nl300679e.
161. Li T.I., Sknepnek R., de la Cruz M.O., J. Am. Chem. Soc., 2013, **135**, No. 23, 8535; doi:10.1021/ja312644h.
162. Auyeung E., Li T., Senesi A.J., Schmucker A.L., Pals B.C., de la Cruz M.O., Mirkin C.A., Nature, 2014, **505**, 73; doi:10.1038/nature12739.
163. Leunissen M.E., Frenkel D., J. Chem. Phys., 2011, **134**, No. 8, 084702; doi:10.1063/1.3557794.
164. Guerrini L., Barrett L., Dougan J.A., Faulds K., Graham D., Nanoscale, 2013, **5**, No. 10, 4166; doi:10.1039/c3nr011.
165. Mognetti B.M., Leunissen M.E., Frenkel D., Soft Matter, 2012, **8**, No. 7, 2213; doi:10.1039/c2sm06635a.
166. Uberti-Angioletti S., Mognetti B.M., Frenkel D., Nat. Mater., 2012, **11**, 518; doi:10.1038/nmat3314.
167. Gang O., Nat. Mater., 2012, **11**, No. 6, 487; doi:10.1038/nmat3344.
168. Di Michele L., Varrato F., Kotar J., Nathan S.H., Foffi G., Eiser E., Nat. Commun., 2013, **4**, 2007; doi:10.1038/ncomms3007.
169. Martinez-Veracoechea F.J., Bozorgui B., Frenkel D., Soft Matter, 2010, **6**, No. 24, 6136; doi:10.1039/c0sm00567c.
170. Martinez-Veracoechea F.J., Mladek B.M., Tkachenko A.V., Frenkel D., Phys. Rev. Lett., 2011, **107**, No. 4, 045902; doi:10.1103/PhysRevLett.107.045902.
171. Hazarika P., Irrgang J., Spengler M., Niemeyer C.M., Adv. Funct. Mater., 2007, **17**, No. 3, 437; doi:10.1002/adfm.200600694.
172. Mladek B.M., Fornleitner J., Martinez-Veracoechea F.J., Dawid A., Frenkel D., Phys. Rev. Lett., 2012, **108**, No. 26, 268301; doi:10.1103/PhysRevLett.108.268301.
173. Rabideau B.D., Bonnecaze R.T., Langmuir, 2007, **23**, No. 20, 10000; doi:10.1021/la701166p.
174. Yanagishima T., Laohakunakorn N., Keyser U.F., Eiser E., Tanaka H., Soft Matter, 2014, **10**, No. 11, 1738; doi:10.1039/c3sm52830h.
175. Schmatko T., Bozorgui B., Geerts N., Frenkel D., Eiser E., Poon W.C.K., Soft Matter, 2007, **3**, No. 6, 703; doi:10.1039/b618028k.
176. Dreyfus R., Leunissen M.E., Sha R., Tkachenko A., Seeman N.C., Pine D.J., Chaikin P.M., Phys. Rev. E, 2010, **81**, No. 4, 041404; doi:10.1103/PhysRevE.81.041404.
177. Rogers B.W., Crocker J.C., Proc. Natl. Acad. Sci. USA, 2011, **108**, No. 38, 15687; doi:10.1073/pnas.1109853108.
178. Mognetti B.M., Varilly P., Angioletti-Uberti S., Martinez-Veracoechea F.J., Dobnikar J., Leunissen M.E., Frenkel D., Proc. Natl. Acad. Sci. USA, 2012, **109**, No. 7, E378; doi:10.1073/pnas.1119991109.
179. Dreyfus R., Leunissen M., Sha R., Tkachenko A., Seeman N., Pine D., Chaikin P., Phys. Rev. Lett., 2009, **102**, No. 4, 048301; doi:10.1103/PhysRevLett.102.048301.
180. Sun Y., Harris N.C., Kiang C.H., Physica A, 2005, **350**, No. 1, 89; doi:10.1016/j.physa.2005.01.013.
181. Park S., Stroud D., Phys. Rev. B, 2003, **68**, 224201; doi:10.1103/PhysRevB.68.224201.
182. Park S., Stroud D., Phys. Rev. B, 2003, **67**, 212202; doi:10.1103/PhysRevB.67.212202.
183. Lazarides A.A., Schatz G.C., J. Chem. Phys., 2000, **112**, No. 6, 2987; doi:10.1063/1.480873.
184. Lazarides A.A., Schatz G.C., J. Phys. Chem. B, 2000, **104**, No. 3, 460; doi:10.1021/jp992179+.
185. Yan Y., Chen J.I., Ginger D.S., Nano Lett., 2012, **12**, No. 5, 2530; doi:10.1021/nl300739n.
186. Séverac F., Alphonse P., Estève A., Bancaud A., Rossi C., Adv. Funct. Mater., 2012, **22**, No. 2, 323; doi:10.1002/adfm.201100763.
187. Busson M.P., Rolly B., Stout B., Bonod N., Larquet E., Polman A., Bidault S., Nano Lett., 2011, **11**, No. 11, 5060; doi:10.1021/nl2032052.
188. Mukundan V.T., Quang M.N.T., Miao Y.H., Phan A.T., Soft Matter, 2013, **9**, No. 1, 216; doi:10.1039/C2SM26652K.
189. Varilly P., Angioletti-Uberti S., Mognetti B.M., Frenkel D., J. Chem. Phys., 2012, **137**, No. 9, 094108; doi:10.1063/1.4748100.
190. Angioletti-Uberti S., Varilly P., Mognetti B.M., Tkachenko A.V., Frenkel D., J. Chem. Phys., 2013, **138**, 021102; doi:10.1063/1.4775806.
191. Tkachenko A.V., Phys. Rev. Lett., 2002, **89**, No. 14, 148303; doi:10.1103/PhysRevLett.89.148303.

192. Tkachenko A.V., Phys. Rev. Lett., 2011, **106**, 255501; doi:10.1103/PhysRevLett.106.255501.
193. Halverson J.D., Tkachenko A.V., Phys. Rev. E, 2013, **87**, No. 6, 062310; doi:10.1103/PhysRevE.87.062310.
194. Zeravcic Z., Manoharan V.N., Brenner M.P., Proc. Natl. Acad. Sci. USA, 2014, doi:10.1073/pnas.1411765111.
195. Licata N., Tkachenko A., Phys. Rev. E, 2006, **74**, No. 4, 040401(R); doi:10.1103/PhysRevE.74.040401.
196. Licata N., Tkachenko A., Phys. Rev. E, 2006, **74**, No. 4, 041406; doi:10.1103/PhysRevE.74.041406.
197. Licata N.A., Tkachenko A.V., Europhys. Lett., 2008, **81**, No. 4, 48009; doi:10.1209/0295-5075/81/48009.
198. Licata N., Tkachenko A.V., Phys. Rev. E, 2009, **79**, No. 1, 011404; doi:10.1103/PhysRevE.79.011404.
199. Jenkins I.C., Casey M.T., McGinley J.T., Crocker J.C., Sinno T., Proc. Natl. Acad. Sci. USA, 2014, **111**, No. 13, 4803; doi:10.1073/pnas.1318012111.
200. Lukatsky D., Frenkel D., Phys. Rev. Lett., 2004, **92**, No. 6, 068302; doi:10.1103/PhysRevLett.92.068302.
201. Lukatsky D.B., Frenkel D., J. Chem. Phys., 2005, **122**, No. 21, 214904; doi:10.1063/1.1906210.
202. Lukatsky D.B., Mulder B.M., Frenkel D., J. Phys.: Condens. Matter, 2006, **18**, No. 18, S567; doi:10.1088/0953-8984/18/18/S05.
203. Jin R., Wu G., Li Z., Mirkin C.A., Schatz G.C., J. Am. Chem. Soc., 2013, **125**, No. 6, 1643; doi:10.1021/ja021096v.
204. Talanquer V., J. Chem. Phys., 2006, **125**, No. 19, 194701; doi:10.1063/1.2370872.
205. Tindemans S.H., Mulder B.M., Phys. Rev. E, 2010, **82**, No. 2, 021404; doi:10.1103/PhysRevE.82.021404.
206. Srinivasan B., Vo T., Zhang Y., Gang O., Kumar S., Venkatasubramanian V., Proc. Natl. Acad. Sci. USA, 2013, **110**, No. 46, 18431; doi:10.1073/pnas.1316533110.
207. Gottwald D., Kahl G., Likos C.N., J. Chem. Phys., 2005, **122**, 204503; doi:10.1063/1.1901585.
208. Fornleitner J., Lo Verso F., Kahl G., Likos C.N., Soft Matter, 2008, **4**, 480; doi:10.1039/b717205b.
209. Doppelbauer G., Bianchi E., Kahl G., J. Phys.: Condens. Matter, 2010, **22**, 104105; doi:10.1088/0953-8984/22/10/104105.
210. Doppelbauer G., Noya E.G., Bianchi E., Kahl G., Soft Matter, 2012, **8**, 7768; doi:10.1039/c2sm26043c.
211. Lee O.S., Schatz G.C., J. Phys. Chem. C, 2009, **113**, No. 6, 2316; doi:10.1021/jp8094165.
212. Ngo V.A., Kalia R.K., Nakano A., Vashishta P., J. Phys. Chem. C, 2012, **116**, No. 36, 19579; doi:10.1021/jp306133v.
213. Knorowski C., Travesset A., J. Am. Chem. Soc., 2014, **136**, No. 2, 653; doi:10.1021/ja406241n.
214. Dhakal S., Kohlstedt K.L., Schatz G.C., Mirkin C.A., de la Cruz M.O., ACS Nano, 2013, **7**, No. 12, 10948; doi:10.1021/nn404476f.
215. Leunissen M.E., Dreyfus R., Sha R., Seeman N.C., Chaikin P.M., J. Am. Chem. Soc., 2010, **132**, No. 6, 1903; doi:10.1021/ja907919j.
216. Noyong M., Ceyhan B., Niemeyer C.M., Simon U., Colloid Polym. Sci., 2006, **284**, 1265; doi:10.1007/s00396-006-1518-3.
217. Cobbe S., Connolly S., Ryan D., Nagle L., Eritja R., Fitzmaurice D., J. Phys. Chem. B, 2003, **107**, No. 2, 470; doi:10.1021/jp021503p.
218. Diaz J.A., Grewer D.M., Gibbs-Davis J.M., Small, 2012, **8**, No. 6, 873; doi:10.1002/smll.201101922.
219. Jayagopal A., Halfpenny K.C., Perez J.W., Wright D.W., J. Am. Chem. Soc., 2010, **132**, No. 28, 9789; doi:10.1021/ja102585v.
220. Leunissen M.E., Dreyfus R., Sha R., Wang T., Seeman N.C., Pine D.J., Chaikin P.M., Soft Matter, 2009, **5**, No. 12, 2422; doi:10.1039/b817679e.
221. Li D., Banon S., Biswal S.L., Soft Matter, 2010, **6**, No. 17, 4197; doi:10.1039/c0sm00159g.
222. Park S.J., Lee J.S.H., Georganopoulos D., Mirkin C.A., Schatz G.C., J. Phys. Chem. B, 2006, **110**, No. 25, 12673; doi:10.1021/jp062212+.
223. Wu K.T., Feng L., Sha R., Dreyfus R., Grosberg A.Y., Seeman N.C., Chaikin P.M., Phys. Rev. E, 2013, **88**, No. 2, 022304; doi:10.1103/PhysRevE.88.022304.
224. Auyeung E., Macfarlane R.J., Choi C.H.J., Cutler J.I., Mirkin C.A., Adv. Mater., 2012, **24**, No. 38, 5181; doi:10.1002/adma.201202069.
225. Radha B., Senesi A.J., O'Brien M.N., Wang M.X., Auyeung E., Lee B., Mirkin C.A., Nano Lett., 2014, **14**, No. 4, 2162; doi:10.1021/nl500473t.
226. Kim Y., Macfarlane R.J., Mirkin C.A., J. Am. Chem. Soc., 2013, **135**, No. 28, 10342; doi:10.1021/ja405988r.

## Самоскупування DNA-функціоналізованих колоїдів

П.Е. Теодоракіс<sup>1</sup>, Н.Г. Фітас<sup>2</sup>, Г. Каль<sup>3,4</sup>, Ч. Деллаго<sup>4,5</sup>

<sup>1</sup> Відділ хімічної інженерії, Емпіріал Коледж Лондон, SW7 2AZ Лондон, Великобританія

<sup>2</sup> Центр Прикладних математичних досліджень, Університет Ковентрі, CV1 5FB, Ковентрі, Великобританія

<sup>3</sup> Інститут теоретичної фізики, Віденський технічний університет, A-1040 Віденський, Австрія

<sup>4</sup> Центр обчислювального матеріалознавства (CMS), A-1040 Віденський, Австрія

<sup>5</sup> Факультет фізики, Університет Відня, A-1090 Віденський, Австрія

Колоїдні частинки з прикріпленими однонитковими DNA (ssDNA) ланцюжками, здатні самоскупуватися у низку різних кристалічних структур, де гібридизація ланцюжків ssDNA створює зв'язки між колоїдами, стабілізуючи їх структуру. Залежно від геометрії і розміру частинок, густини прищеплених ланцюжків ssDNA, а також густини та вибору послідовностей DNA, можна виготовляти низку різних кристалічних структур. Однак залишається незрозумілим і потребує інтенсивних досліджень питання, яким чином ці фактори роблять синергетичний внесок у процес самоскупчення DNA-функціоналізованих частинок нано- або мікророзмірів. Більше того, додаткові труднощі для розв'язання даної проблеми полягають у виготовленні далекосяжних структур завдяки кінетичним критичним елементам при самоскупченні. У статті обговорюються найновіші досягнення теорії та експерименту з особливим наголосом на останні дослідження методами комп'ютерного моделювання.

**Ключові слова:** DNA-функціоналізовані наночастинки, самоскупчення, експеримент, теорія, комп'ютерне моделювання